Durability of a Magnetorheological Fluid in a Prosthetic Knee Joint

Einar Hreinsson

Faculty of Industrial Engineering, Mechanical Engineering and Computer Science
University of Iceland
2011

DURABILITY OF A MAGNETORHEOLOGICAL FLUID IN A PROSTHETIC KNEE JOINT

Einar Hreinsson

60 ECTS thesis submitted in partial fulfillment of a
Magister Scientiarum degree in Mechanical Engineering

Advisors
Fjóla Jónsdóttir
Ketill Heiðar Guðmundsson

Faculty Representative
Ragnar Sverrisson

Faculty of Industrial Engineering, Mechanical
Engineering and Computer Science
School of Engineering and Natural Sciences
University of Iceland
Reykjavik, May 2011

Durability of a Magnetorheological Fluid in a Prosthetic Knee Joint
Durability of magnetorheological fluids
60 ECTS thesis submitted in partial fulfillment of a M.Sc. degree in Mechanical Engineering

Faculty of Industrial Engineering, Mechanical
Engineering and Computer Science
School of Engineering and Natural Sciences
University of Iceland
VRII, Hjardarhagi 2-6
107, Reykjavik, Reykjavik
Iceland

Telephone: 525 4000

Bibliographic information:
Einar Hreinsson, 2011, Durability of a Magnetorheological Fluid in a Prosthetic Knee Joint, M.Sc. thesis, Faculty of Industrial Engineering, Mechanical Engineering and Computer Science, University of Iceland.

Printing: Háskólaprent, Fálkagata 2, 107 Reykjavík
Reykjavik, Iceland, May 2011

Abstract

The durability of a magnetorheological (MR) fluid is a problem in a commercially available MR fluid device. This device is a prosthetic knee joint equipped with an MR rotary brake actuator that utilizes the MR fluid in direct-shear mode. After long periods of usage, the actuator becomes stiff in off-state mode and eventually needs to be replaced by a new actuator. The reasons behind the increased off-state rotary stiffness and the degradation of the MR fluid are investigated. MR fluids from used actuators are analysed, after an actual usage by an amputee or after an excitation in a test-rig. Energy dissipated by the fluid in the actuator over its life time is calculated and compared to recognized durability threshold for the in-use-thickening of MR fluids. The energy does not reach this threshold but the durability is still considered relatively good. The powders are extracted from the base fluid. Their morphology, size distribution, chemical composition and magnetic characteristics are analysed and compared to that of unused powder. The chemical composition of used base fluids are analysed and compared to that of an unused base fluid. Results indicate that the iron particles tend to fracture and the surface tends to spall. Thin flakes peel away from the surface and are believed to cause agglomeration resulting in thickening of the fluid. Oxidation or formation of nano-sized particles is not observed in the fluid. Alternative fluid compositions are prepared and tested but do not turn out to be superior with respect to durability.

Útdráttur

Ending segulvökva (e. magnetorheological fluid) hefur verið vandamál í ákveðnu stoðtæki. Tæki þetta er gervihné sem byggir á segulvökvabremsu og notar segulvökvann í skerálagi. Með tímanum stífnar bremsan upp og verður að lokum ónothæf og þarf þá að skipta um hana. Þessi ritgerð lýsir þeirri vinnu sem fólst í því að greina endingu segulvökvans og rannsaka ástæður þess að gæði hans minnka með tímanum. Notaðir segulvökvar eru rannsakaðir og bornir saman við ónotaða. Fylgst er með því hvernig gæði vökvans minnkar með prófunum í þar til gerðu tæki. Orkan sem vökvinn tekur upp á líftíma sínum er reiknuð og borin saman við þekkt mörk fyrir endingu MR vökva. Reiknuð orka nær ekki þessum mörkum en endingin er engu að síður álitin mjög góð. Vökvinn þykknar með tímanum og unnið er að því að greina ástæður þess. Járnduft er aðskilið frá vökvanum. Lögun, stærðardreifing, efnasamsetning og seguleiginleikar notaðra járnagnanna eru rannsakaðir og bornir saman við nýjar agnir. Efnasamsetning grunnvökvans er einnig mæld. Niðurstöður sýna að yfirborð járnagnanna brotnar og þunnar skeljar flagna af yfirborðinu. Þessar þunnu skeljar eru taldar loða saman í vökvanum og valda því að hann þykknar. Ryðmyndun virðist ekki eiga sér stað í mælanlegu magni og ekki er áberandi mikið um agnir af nanó-stærð. Nýjar vökvablöndur eru prófaðar og bornar saman með tilliti til endingar en af því sem prófað var kom núverandi vökvi best út.

Contents

List of Figures

List of Tables

Abbreviations

- **MR** : Magnetorheological
- **CIP** : Carbonyl Iron Powder
- **PSD** : Particle Size Distribution
- **SEM** : Scanning Electron Microscope
- **EDS** : Energy Dispersive X-Ray Spectroscopy
- **LALLS** : Low Angle Laser Light Scattering
- **VSM** : Vibrating Sample Magnetometer

- **On-state** : Under the influence of a magnetic field
- **Off-state** : In the absence of a magnetic field

Acknowledgments

This thesis summarises work and conclusions on the analysis of MR fluid durability in a prosthetic knee joint. This work is a part of my MSc program in Mechanical Engineering at the University of Iceland. Many good people kindly gave their support in the one year period of the project. First of all I would like to thank my supervisors, Prof. Fjóla Jónsdóttir and PhD student Ketill Heiðar Guðmundsson at the Uni. of Iceland for all their support and encouragement during this project. I want to thank R&D Engineer Andrew Bache, R&D Engineer Stefán Páll Sigþórsson, Manufacturing Engineer Björn Sighvatsson, Rheo Technician Binh The Duong and all the other staff at Össur hf. that supported me with work and valuable advices during this project. I would like to thank BSc student Hörður Sæmundsson at VIA University College for his cooperation in torque measurements. I want to thank Project Manager Birgir Jóhanesson at Innovation Center Iceland for good cooperation when operating the microscope. Special gratitude goes to Prof. Antonio J. F. Bombard at Itajubá Federal University in Brazil, who performed many measurements when available equipment in Iceland was inadequate. I would also like to thank Research Engineer John Ulicny at General Motors for his advices on measuring techniques. This project is funded by the Icelandic Centre for Research, grant no. 090035022, and by Össur hf.

1 Introduction

1.1 Background

A group of materials which respond to an external stimulus by change in material properties are called smart materials. The stimulus can be temperature, pressure, light, pH value, electric field, magnetic field etc. and the result can be variation in shape, volume, voltage, colour, apparent viscosity or other material properties (Shahinpoor and Schneider, 2008). Examples of smart materials in the form of fluids are magnetorheological (MR) fluids, electrorheological (ER) fluids and ferrofluids, all of whose rheological properties can be controlled by an external stimulus. ER fluids undergo a change in apparent viscosity in the presence of an electric field while the apparent viscosity of ferrofluids and MR fluids is controlled by a magnetic field. Ferrofluids are colloidal fluids consisting of suspensions of nano-sized magnetizable particles in a nonmagnetic carrier fluid (Rosensweig, 1987). MR and ER fluids, on the other hand, are prepared by suspending micron-sized magnetizable particles in a nonmagnetic base fluid such as oil (Shahinpoor and Schneider, 2008).

The durability of MR fluids has been drawn to the attention of researchers during the last decade (Carlson, 2002, 2003; Golden et al., 2005; Smith et al., 2007; Ulicny et al., 2007a,b). Carlson (2002) has defined good features that an MR fluid needs to exhibit; one of those features relating to durability. All MR fluids will eventually show some deterioration, the best known is the increase in fluid viscosity after long periods of usage. It is referred to as in-use-thickening (IUT) and has been identified and stated as solved (Carlson, 2002). A stated upper limit for the energy that a good MR fluid can dissipate over its lifetime is $10^7 J/cm^3$ (Carlson, 2002). Durability of MR fluids was not identified as a serious problem until MR fluids were applied in devices in which the fluid is continuously excited with high loads, for long periods of time. Examples of such applications are vehicle systems seat dampers (Carlson, 2003) and fan clutches (Golden et al., 2005; Smith et al., 2007). The MR fluid in a fan clutch is used to transmit a variable torque between a motor and a fan resulting in fast controllability. A clutch application imposes a continuous force on the MR fluid while the fan is active. This relies heavily on the durability of the employed MR fluid.

Several causes are known for IUT depending on the fluid formulation. When mechanically hard particles are subjected to prolonged high stresses the surface layer fractures and breaks into secondary particles (Carlson, 2002). Irregular shape of the secondary particles can cause them to adhere to one another resulting in particle agglomeration and fluid thickening (Iyengar and Foister, 2003). The secondary particles can be nano-sized or break down into nano-sized particles due to their shape and brittleness. Addition of nanometer-sized particles significantly increases the off-state viscosity of MR fluids due to large surface to weight ratio (Carlson, 2002; Jonsdottir and Gudmundsson). Softer particles such as reduced carbonyl iron powder tend to flatten out rather than fracture and break when subjected to high stresses. This too affects the rheological characteristics of the fluid since the flattened and deformed particles adhere to one another and cause agglomeration(Iyengar and Foister, 2003). Fumed silica fluid stabilizing additive can cause similar effects under high loads. The fumed silica particles can mechanically bond to the iron particles which can accelerate agglomeration (Iyengar and Foister, 2003). A different mechanism that increases the off-state viscosity is polymerization of the base fluid. The exposure of additional iron surfaces when the particles flatten or break can accelerate the polymerization of the base fluid molecules by catalysis and free radical mechanisms (Iyengar and Foister, 2003)
Other type of fluid degradation is the decrease in ability to withstand shear stress in the presence of a magnetic field. An example of mechanism causing this type of degradation is oxidation of the magnetizable particles. Oxidation reduces the MR effect of the fluid since iron oxides exhibit poorer magnetic properties than pure iron. This has shown to decrease the overall MR effect of more than 20% (Iyengar et al., 2004).

Various solutions have been developed to increase the durability of MR fluids, depending on the application and the mechanism responsible for the degradation. Munoz (1997) describes an MR fluid composition that exhibits superior durability due to substantial decrease in IUT. This composition consist of high purity iron particles (mechanically soft), a carrier fluid and thiophosphorous and/or thiocarbamate additives. In another MR fluid patent, Munoz et al. (1997) describe high purity iron particles of reduced CIP as particularly preferred particle material for a durable MR fluid. Organomolybdenum is presented as a durability increasing additive in the same composition. Karol et al. (1999) present an MR fluid composition consisting of mechanically soft reduced CIP in a carrier fluid and at least one phosphorus additive such as phosphonate, phosphonite, phosphate, phosphinate, phosphinite, phosphite or corrisponding amide or imide. Weiss et al. (1995) describe an MR fluid consisting of particles in a carrier fluid and a thixotropic additive as a stabilizing agent. A mixture of reduced CIP and iron oxide powder is preferred as the particle component. The iron oxide powder is believed to remove corrosion products from the surface of the CIP and enhance magnetic properties of the fluid.
Mechanically soft and compressible particles of CIP are by many considered preferable with respect to durability due to the abrasive surface of the mechanically hard particles. However, Iyengar and Foister (2003) consider mechanically hard particles as preferred in a durable MR fluid composition for high compression dampening devices. Particles

of mechanically soft CIP are shown to deform when subjected to long term stress. The carrier fluid is a mixture of polyalphaolefin and a plasticizer and the composition includes unreduced fumed silica as a thixotropic agent.
Golden et al. (2005) describe an MR fluid composition utilizing CIP of bimodal size distribution. The powder is a mixture of reduced (mechanically soft) and unreduced (mechanically hard) carbonyl iron. The composition utilizes alpha olefin oil as a base fluid and fumed silica as a suspending agent. Molybdenum amine is preferred as a friction- and oxidation reducing additive. Zinc dialkyl dithiophosphate (ZDDP) is additionally presented to reduce friction and the effect of IUT. Ulicny et al. (2005) present an MR fluid of improved durability, utilizing mechanically soft and hard CIP of bimodal size distribution suspended in hydrocarbon oil. Fumed silica is utilized as a suspending agent and stearate and thiophosphate additives utilized to reduce friction and increase the durability. Klingenberg et al. (2010) also describe a durable fluid consisting of same powders but including surface active additives of lithium 12-hydroxy stearate (LiHS) and zinc-o,o-di-n-butylphosphorodithiolate (ZBPD) to reduce drag over time. Ulicny et al. (2007a) introduce the use of colloidal polytetrafluoroethelyne or colloidal graphite, along with mechanically hard particles in polyalphaolefin oil to inhibit surface-to-surface contact and scuffing of the particles.
While friction-reducing additives may increase the long-term durability of the fluid, some of them may have negative effects on the off-state viscosity or on-state performance. Many of the friction-reducing additives are toxic which is highly inadvicable in most applications. Also, increasing the number of different materials in the fluid composition may increase the production time and cost. The use of water atomized iron particles having a passivating oxide layer of iron oxide and at least one alloying metal oxide has shown to have slower oxidation as well as higher shear stress and lower viscosity than pure carbonyl iron (Foister et al., 2004). Martensitic or ferritic stainless steel particles can be used instead of carbonyl iron in applications where oxidation resistance and high mechanical strength are critical properties (Iyengar et al., 2004).

1.2 Motivation and goals

This project is focused on MR fluid in a certain commercial device, a prosthetic knee joint described in Chapter 2. The effectiveness of the knee joint decreases as the knee is used and this degradation is believed to be directly related to degradation of the MR fluid. The MR fluid is subjected to high shear stress in micron sized gaps between steel blades. The micron sized gaps limit the choice of particles being used in the fluid. The small blade gaps also result in very high shear rates. The volume of MR fluid is small to limit the size and weight of the device. Due to small fluid volume and continuous excitement of the fluid, the amount of mechanical energy dissipated by the fluid over its lifetime is very high. Eventually the knee needs to be sent back to the manufacturer where the knee joint is replaced or re-built. This causes inconvenience for the user and is costly for the

manufacturer. Increased durability of the MR fluid is therefore important to increase the comfort for the amputee and reduce cost for the manufacturer. The aim of this project is to evaluate the durability of the MR fluid used in the application described above, identify the cause of fluid degradation and develop possible solution to increase the durability.

1.3 Overview of the thesis

The prosthetic knee joint is described in Chapter 2. The effect of temperature on knee joint stiffness is measured to obtain the minimum ambient temperature for usage. Current through the coil and knee joint angle are measured as a function of time in actual usage and the on-state torque is measured for different values of coil current. The results are used to calculate the lifetime dissipated energy (LDE) of the fluid in the device. Properties and characteristics of the MR fluid are described and different fluid compositions compared. Chapter 3 describes tests performed on new actuators. The effect of high temperatures, current and mechanical friction on actuators is analysed. A durability test is performed to evaluate and compare the durability of different fluid compositions. Off- and on-state torque of the actuators are monitored during the tests and the results presented. Used and unused MR fluids are analysed in Chapter 4. The fluids are analysed after an actual usage by an amputee or after an excitation in a test-rig. A method developed to extract the magnetizable particles from the base fluid is described. Used base fluids and particles are then analysed separately and compared to unused. Particle morphology, size distribution and magnetic characteristics is measured. Elemental composition of the particles and base fluid is measured separately. Conclusions are presented in Chapter 5.

2 Magnetorheological (MR) prosthetic knee

The prosthetic knee joint motivating this work is described in this chapter. Relationship between MR fluid properties and MR actuator torque is calculated. The minimum operating temperature is derived from the relationship between temperature and actuator torque. The relationship between coil current and braking torque is measured. The coil current and knee joint angle are measured as a function of time while an amputee walks. The results are used to calculate the lifetime dissipated energy of the fluid in the device. The MR fluid is described, its properties and characteristics in the actuator. Alternative fluid compositions are introduced, tested and compared to the currently used composition.

2.1 An MR rotary brake actuator

An application of MR fluid in direct shear mode is a prosthetic knee-joint manufactured by Össur hf. (2011) and shown in Figure 2.1. The knee joint is equipped with an MR rotary disk type brake actuator in which the fluid is sheared between a stack of steel blades. The blades are attached alternately to the inner housing (rotor) and outer housing (stator) of the knee joint. The outer housing is constructed of nickel-coated aluminium and is connected to the amputee's residual limb. The inner housing is constructed of titanium and connected to the lower part of the knee. The blade stack has a total of 63 blades and the gap between the blades is approximately 25μm (Jonsdottir et al., 2009). The geometry of the actuator has been optimized to maximize the effectiveness of the MR fluid (Jonsdottir et al., 2009).

A coil around a Co-Fe core in the center of the actuator produces the magnetic field. The braking torque in the actuator is controlled by varying the current through the coil. A microprocessor reads signals from an angle sensor and load-cells located in the knee and actively controls the current through the coil. A spring located at one side of the actuator pulls the knee into upright position when load is released.
For this application, it is desirable for the on-state torque to be as high as possible to ensure sufficient braking torque, and for the off-state torque to be as low as possible to

ensure sufficient smoothness, flexibility and swing extension. The effectiveness of the MR fluid can be evaluated by the turn-up ratio which is defined as the ratio of on-state shear yield stress to off-state viscosity. The off-state torque tends to increase as the knee is used, which results in reduced swing extension. Eventually, the swing extension becomes inacceptable and the knee joint needs to be replaced or re-built. The on-state torque decreases at the same time, reducing the effectiveness and turn-up ratio for the fluid.

Figure 2.1: Rheo knee®, a product from Össur hf. (2011)

2.1.1 Relating actuator torque and fluid properties

The MR actuator must be disassembled in order to measure the viscosity μ of the fluid inside it. Measuring the viscosity requires the use of a viscometer that is not available in Iceland. Instead of measuring the viscosity directly, it was calculated theoretically from measured actuator stiffness. Similarly, the shear yield stress τ_{yield} of the fluid was calculated from the on-state actuator torque. Using this method the fluid viscosity and shear yield stress can be estimated quickly and repeatedly. However, this method is not as accurate as measuring the viscosity directly.
Figure 2.2 illustrates how the fluid is subjected to simple shear between parallel rotating blades in the knee actuator. Constants and variables are listed below. T_{fric} is the torque due to friction in seals and bearings, measured on an empty actuator at approximately $\pi/4$ rad/s. R_o and R_i are the effective inner and outer radii of the steel blades and L is the gap between them.

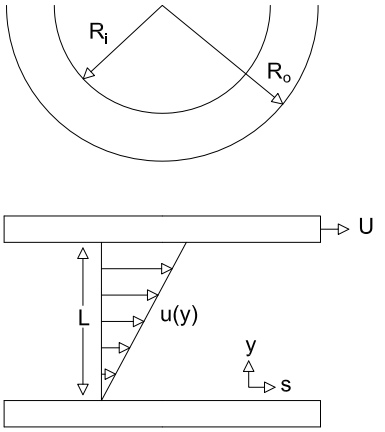

Figure 2.2: Fluid in simple shear

Variables:

T	:	Measured torque
ω	:	Angular velocity
τ	:	Shear stress
μ	:	Viscosity

Constants:

$T_{fric} = 0.4Nm$	:	Frictional torque
$R_i = 18.2mm$	:	Inner radius of blades
$R_o = 24.2mm$	:	Outer radius of blades
$L = 25\mu m$	:	Blade gap
$n = 62$	:	Number of blade gaps

Assuming laminar flow and linear velocity profile:

$$\begin{aligned} \frac{d^2u}{dy^2} &= 0 \\ u &= 0 \text{ at } y = 0 \\ u &= U \text{ at } y = L \\ \Rightarrow u &= y/L \cdot U \end{aligned}$$

Active blade area:

$$A = \int_{R_i}^{R_o} 2\pi r\, dr$$

The shear stress due to viscosity in the fluid:

$$\tau_{visc} = \mu \cdot U/L = \mu \cdot (r \cdot \omega)/L$$

Shear force due to viscosity at a given radius:

$$F_{visc}(r) = \tau_{visc} \cdot dA = \mu \cdot (r \cdot \omega)/L \cdot 2\pi \cdot r$$

Torque effect at a given radius is the product of shear force and radius. Actuator torque due to fluid viscosity in off-state mode is found by integrating the torque from inner to outer blade radius and multiplying by number of blade gaps:

$$T_{visc} = \int_{R_i}^{R_o} r \cdot F(r)\, dr = \frac{\pi \cdot \mu \cdot \omega \cdot n}{2L} \cdot (R_o^4 - R_i^4) \tag{2.1}$$

Adding frictional torque to the viscous torque in Equation 2.1 and solving for viscosity gives Equation 2.2. This equation can be used to estimate fluid viscosity from measured actuator torque in off-state mode.

$$\mu_{visc} = \frac{2L \cdot (T_{visc} - T_{fric})}{\omega \cdot \pi \cdot (R_o^4 - R_i^4) \cdot n} \tag{2.2}$$

The on-state actuator torque at yield point T_{yield} is calculated from the fluid shear yield stress τ_y (see Section 2.2.1 and Figure 2.7(a) for yield point of MR fluids).

$$\begin{aligned} T_{yield} &= \int_{R_i}^{R_o} r \cdot \tau_y \cdot n \, dA \\ &= 2\pi \int_{R_i}^{R_o} r^2 \cdot \tau_y \cdot n \, dr \\ &= \frac{2\pi \cdot \tau \cdot n}{3} \cdot (R_o^3 - R_i^3) \end{aligned} \tag{2.3}$$

Adding frictional torque and solving for shear yield stress gives Equation 2.4 which can be used to estimate fluid shear yield stress from measured on-state actuator torque at yield point:

$$\tau_{yield} = \frac{T_{yield} - T_{fric}}{2/3\,\pi \cdot (R_o^3 - R_i^3) \cdot n} \tag{2.4}$$

On-state actuator torque at given shear-rate, viscosity and yield stress is obtained by combining Equations 2.1 and 2.3:

$$T_{on}(r) = \frac{\pi \cdot \mu \cdot \omega \cdot n}{2L} \cdot (R_o^4 - R_i^4) + \frac{2\pi \cdot \tau \cdot n}{3} \cdot (R_o^3 - R_i^3) \tag{2.5}$$

2.1.2 Operating temperature range

The knee joint stiffness increases with time and number of cycles but it is also strongly dependent on temperature. The viscosity of the base fluid varies with temperature although the PFPE oil has a relatively high viscosity index compared to other lubricating oils. There is therefore not only a maximum number of cycles or years that the knee joint can last but also a minimum ambient temperature for operation. This minimum temperature then increases with number of cycles and when it has reached common ambient temperature the knee joint needs to be replaced.
To derive the minimum ambient temperature for a new Rheo Knee® (Össur hf. (2011)) the off-state torque was measured for varying temperatures from 8.5 to 35.0°C. The torque was measured at an angular speed of 1.7 rad/s. The measurements were carried out in cooperation with BS student Hörður Sæmundsson and his studies on measurement devices. The results are plotted in Figure 2.3. The different markers show how the torque changes as the knee joint warms up by cycling (without current applied to the coil). The off-state torque decreases strictly with increasing temperature if one outlier at 22°C is omitted. The actuator was stored for a longer time before that particular measurement which is believed to have caused particle settling.

In production and service, the stiffness of new and used knee joints is evaluated by measuring the swing extension, i.e. the angle that the foot travels forward due to gravity when released from a certain angle. These measurements are performed at room temperature ranging from 22-24°C. The minimum swing extension criteria is 39° for new production knees and 32° for used service knees after 50 cycles warm-up. 39° swing extension corresponds to 1.2Nm off-state torque and 32° swing extension corresponds to 1.6Nm off-state torque. The off-state torque criteria for used knees in service can be taken as the maximum off-state torque for a knee joint to operate normally. The minimum operating temperature can then be found using Figure 2.3. The 2nd degree polynomials in Equations 2.6 and 2.7 fit to the set of data points for measurements before and after 50 cycles, respectively. T denotes the off-state actuator torque in Newton-meters and t is the temperature on Celsius scale. The coefficients of determination are shown after each polynomial. Solving Equation 2.7 for T=1.6Nm gives 11°C as the minimum temperature for new knees to function normally. The effect of temperature on on-state torque is much less and considered negligible.

$$\text{0 cycles: } T = 5.23 \cdot 10^{-3} t^2 - 3.03 \cdot 10^{-1} t + 5.3 \qquad R^2 = 0.994 \tag{2.6}$$

$$\text{50 cycles: } T = 1.04 \cdot 10^{-3} t^2 - 9.39 \cdot 10^{-2} t + 2.5 \qquad R^2 = 0.996 \tag{2.7}$$

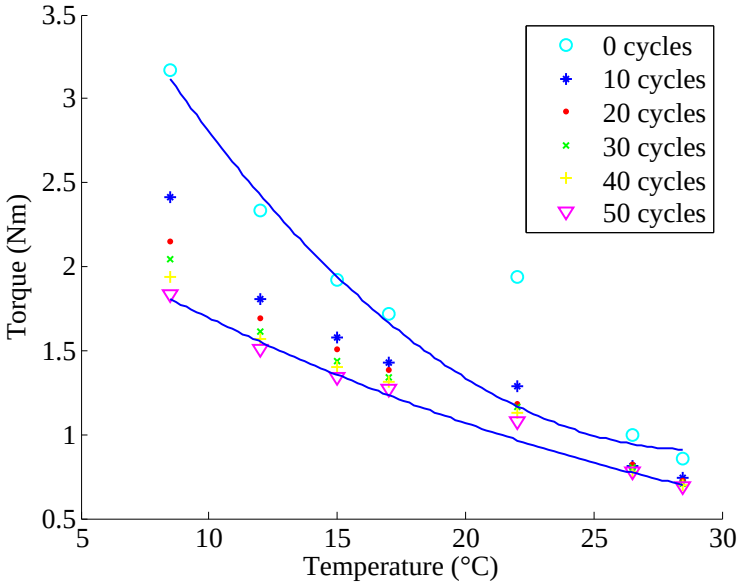

Figure 2.3: The effect of temperature on off-state torque

2.1.3 Effect of coil current on braking torque

The relationship between coil current and on-state torque of the knee joint actuator has been derived theoretically and measured up to 1.5A, which until now has been the maximum coil current in the actuator (Thorarinsson). A new type of microcomputer in the prosthetic knee allows for current amplitudes above 1.5A (see table 2.1). Theoretically, the increase in on-state torque with increased coil current should be relatively small above 1.5A (Thorarinsson). Since this has not been shown experimentally before, the mechanical braking torque of the actuator was measured for varying coil current up to 2.0A. The measurement was performed at ambient temperature of 23°C. A new actuator from Rheo Knee® (Össur hf. (2011)) was used for the experiment. Spring was not removed from the actuator during the experiment. The torque was measured for nine values of current ranging from 0.0 to 2.0A. The current was held constant during each measurement. The torque was measured using a custom device. An electric motor connected to a computer turns the knee joint at a constant angular speed of 0.44 rad/s for various coil currents. A computer software reads data from the motor and returns the torque applied in each case. The knee joint was degaussed between each measurement.

Figure 2.4 shows the relationship between coil current and measured on-state torque at 0.44 rad/s. The dashed line shows a 5th degree polynomial fitted to the data points and used later to estimate how the mechanical torque varies with time in actual usage (see Section 2.1.4).

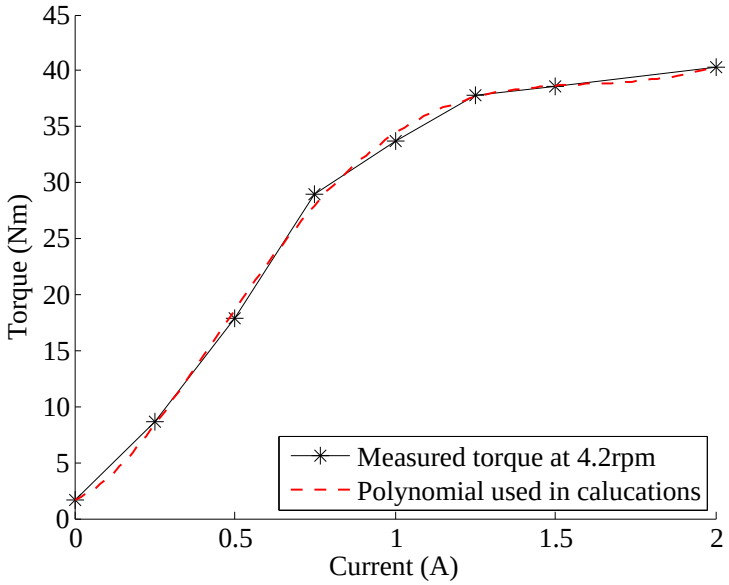

Figure 2.4: The effect of coil current on braking torque

2.1.4 Lifetime dissipated energy

All MR fluids will eventually show some degree of degradation. The knee joint patent states that the actuator should last for $3 \cdot 10^6$ cycles (Hsu et al., 2006). However, after less than 10^6 cycles, the effect of IUT has made the MR fluid unusable. In its lifetime, the fluid is subjected to high shear forces, high shear rates, temperature fluctuations etc. The aim of this section is to seek to evaluate whether 10^6 cycles can be considered as good durability and if $3 \cdot 10^6$ cycles is a realistic aim. A known benchmark is needed to evaluate the quality of the fluid with respect to durability. One benchmark is the lifetime dissipated energy (LDE) defined by Carlson (2002). LDE is a measure of mechanical power converted to heat by a volume of fluid over its lifetime, see Equation 2.8.

$$LDE = \frac{1}{V} \int_0^{life} P \cdot dt \tag{2.8}$$

V denotes the MR fluid volume and P is the mechanical power at each instance. Carlson (2002) states that the best MR fluids today can sustain a LDE on the order of $10^7 J/cm^3$. LDE of the MR fluid in the prosthetic actuator will now be calculated.

The effective volume V of fluid that is sheared between the blades is defined by:

$$V = n \cdot L \cdot (R_o^2 - R_i^2) \cdot \pi = 1.2cm^3 \tag{2.9}$$

The mechanical power $P(t)$ is the product of mechanical torque and angular speed. Mechanical torque can be estimated by measuring the coil current and substituting into the polynomial in figure 2.4. Angular speed is easily derived from measured angle. The coil current and knee joint angle are logged as a function of time while an amputee walks, both on level surface and down stairs. Measured coil current and angle is shown in Figures 2.5(a)-2.5(d). Table 2.1 summarizes the minimum, maximum and mean values of current, angle and angular speed through one cycle.

Substituting the measured coil current in Figures 2.5(a) and 2.5(c) into the polynomial in Figure 2.4 gives the torque in Figures 2.6(a) and 2.6(c), respectively. Multiplying by the angular speed, derived from figures 2.5(b) and 2.5(d), gives the mechanical power shown in Figures 2.6(b) and 2.6(d). Table 2.2 summarizes the mean and maximum values of torque and power through one cycle. The lifetime of the fluid, shown in Table 2.3, is the mean duration of one cycle times the number of cycles.

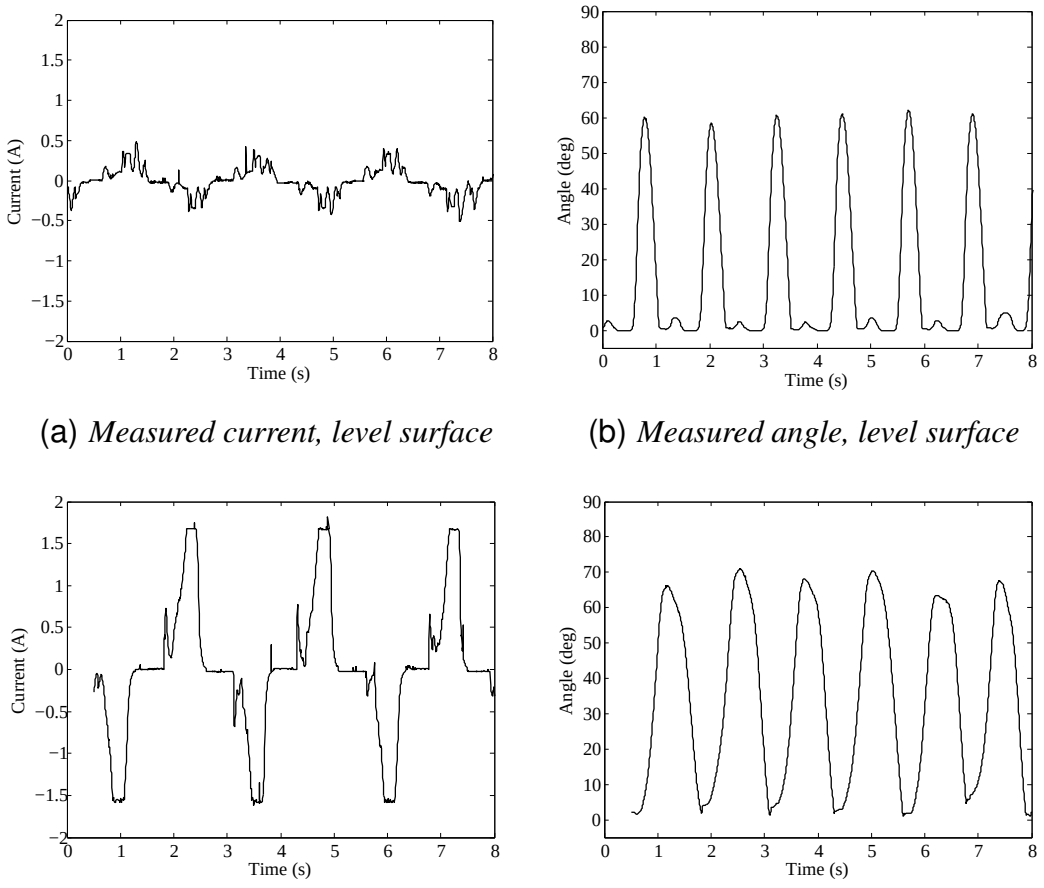

(a) *Measured current, level surface*

(b) *Measured angle, level surface*

(c) *Measured current, down stairs*

(d) *Measured angle, down stairs*

Figure 2.5: Measured coil current and knee angle

Table 2.1: Summary of values for coil current, angle and angular speed

	Level surface	**Down stairs**
Max current	0.52 A	1.82 A
Mean current	0.12 A	0.50 A
RMS current	0.16 A	0.80 A
Max angle	62.0 deg	71.1 deg
Min angle	-0.2 deg	0.9 deg
Max angular speed	8.9 rad/s	5.0 rad/s
Mean angular speed	1.8 rad/s	1.9 rad/s
RMS angular speed	2.9 rad/s	2.3 rad/s

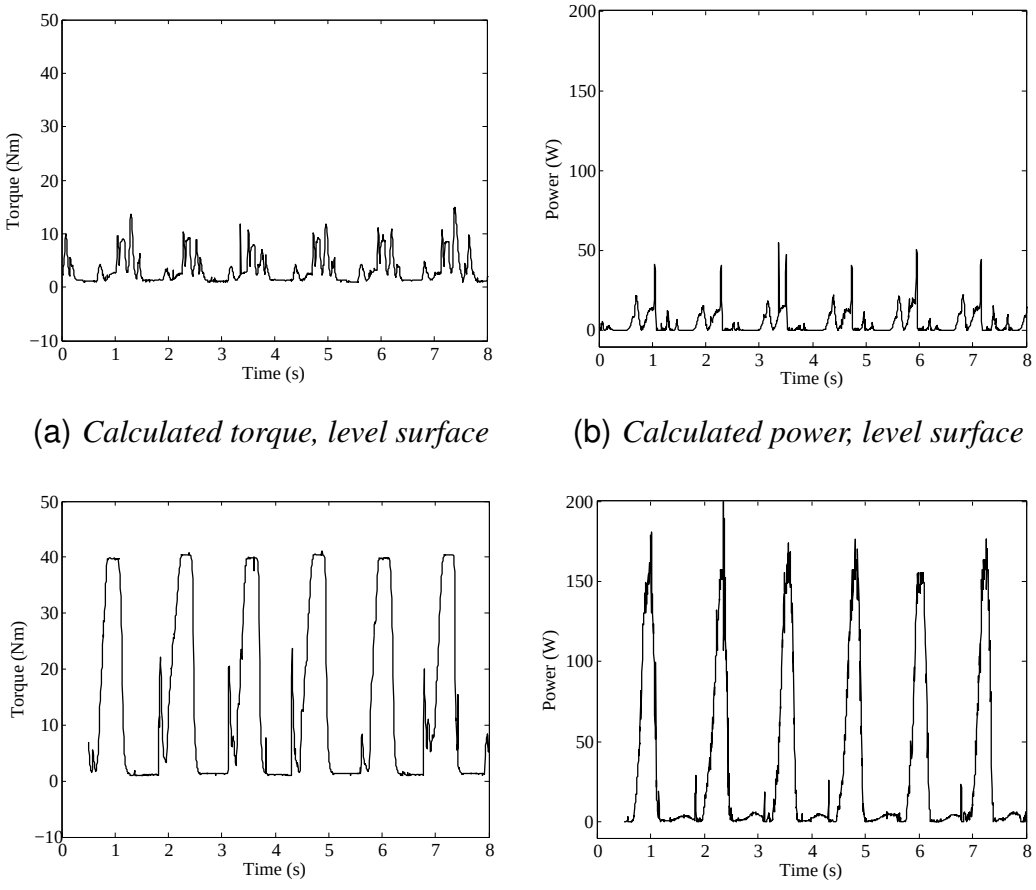

(a) *Calculated torque, level surface*

(b) *Calculated power, level surface*

(c) *Calculated torque, down stairs*

(d) *Calculated power, down stairs*

Figure 2.6: Calculated torque and power

Table 2.2: Summary of calculated power and torque values

	Level surface	**Down stairs**
Max torque	19.2 Nm	39.3 Nm
Mean torque	4.6 Nm	14.8 Nm
RMS torque	5.8 Nm	21.3 Nm
Max Power	71.9 W	193.9 W
Mean Power	6.4 W	34.1 W
RMS Power	11.4 W	61.0 W

Table 2.3: Mean cycle duration on level surface and down stairs

Cycle duration	**1 cycle**	**3 million cycles**
Level surface	1.18 s	$3.54 \cdot 10^6$ s
Down stairs	1.25 s	$3.75 \cdot 10^6$ s

Now all the necessary values have been obtained and the LDE can be calculated according to Equation 2.8. The results are presented in table 2.4. LDE for walking only on level surface for $3 \cdot 10^6$ cycles reaches above the threshold stated by Carlson (2002). For walking down stairs the LDE reaches one order of magnitude higher. An average for most users is believed to be close to pure level surface walking. It is concluded that $3 \cdot 10^6$ cycles is a rather unrealistic goal. LDE for 10^6 cycles is below the threshold stated by Carlson (2002).

Table 2.4: Mechanical energy dissipated by the MR fluid

LDE	$\mathbf{1 \cdot 10^6}$ **cycles**	$\mathbf{3 \cdot 10^6}$ **cycles**
Level surface	$6.2 \cdot 10^6 J/cm^3$	$1.9 \cdot 10^7 J/cm^3$
Down stairs	$3.3 \cdot 10^7 J/cm^3$	$9.8 \cdot 10^7 J/cm^3$

2.2 MR fluid

2.2.1 Characteristics of the MR fluid

In the absence of a magnetic field (off-state mode) the magnetizable particles in an MR fluid are evenly distributed over the fluid volume and do not restrict the fluid flow. The fluid exhibits shear thinning behaviour, that is the viscosity decreases with increasing shear rate as shown in Figure 2.7(a). In the presence of an external magnetic field (on-state mode) the particles acquire dipole moments. If the field strength is sufficient the particles line up in the direction of the magnetic field and form chains or columns (Furst and Gast, 2000). This dramatically increases the apparent viscosity of the fluid, and the fluid becomes a viscoelastic solid (Harris, 1977). At a certain value of stress, the chains of particles start to break and yielding occurs, as seen in figure 2.7(b). This process is completely reversible. Different fluid behaviour models are shown in Figure 2.8. The Bingham plastic model can be used to describe the on-state characteristics of an MR fluid.

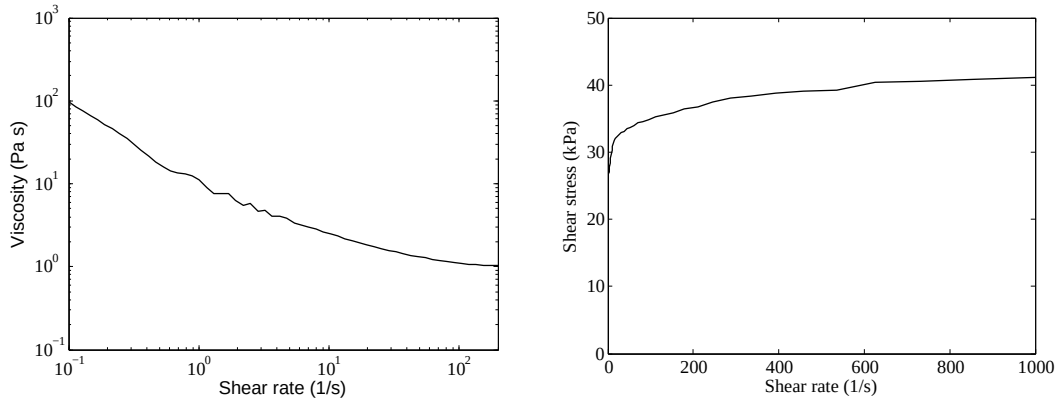

(a) *Viscosity in off-state mode* (b) *Shear stress at 1.5A coil current*

Figure 2.7: Viscosity and shear stress in off- and on-state mode, respectively, as a function of shear rate. Measured by Gudmundsson et al. (2011)

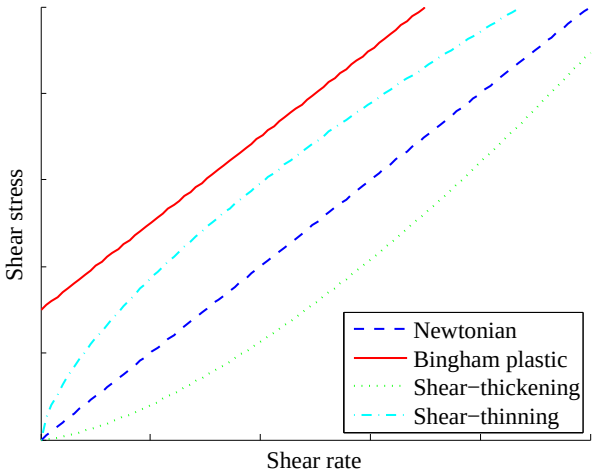

Figure 2.8: Shear stress characteristics of different fluids (Crowe et al., 2005)

Ideally, the magnetizable particles would have zero coercivity, i.e. the particles would be perfectly de-magnetized at the removal of magnetic field. In real world however, the particles gradually become magnetized in the absence of a magnetic field. This causes the off-state viscosity of the fluid to rise and reduces the overall performance. To reverse this effect, an oscillating magnetic field with a decreasing amplitude is applied to the fluid. This is referred to as degaussing and effectively reduces and randomizes the dipole moments of the particles. Stirring the fluid while and after degaussing helps to reverse the magnetic build-up and minimize the off-state viscosity.

2.2.2 Magnetizable particles

Particles in MR fluids should be micron-sized of ferromagnetic material. They preferably have a high magnetic saturation but low coercive force i.e. magnetically soft. Carbonyl iron is the most commonly used material in MR fluid particles, but iron-cobalt, stainless steel, water-atomized iron and other materials have been used for the same purpose. CIP is produced by thermal decomposition of iron pentacarbonyl. Mechanically hard carbonyl iron particles are produced from the primary decomposition products without further chemical processing (BASF (2010)). They have an onion-skin structure as shown in Figure 2.9(a). Iron content is typically around 97.5% and other elements are mainly carbon, nitrogen and oxygen, in this decreasing order. Mechanically soft particles are produced by annealing of hard grades under hydrogen (BASF (2010)). They have polycrystalline structure as shown in Figure 2.9(b) and iron content up to 99.8%.
The particles used in the Rheo Knee® (Össur hf. (2011)) actuators are commercially available micron-sized CIP from BASF (2010). The particles are of type HS which are mechanically hard unreduced CIP.

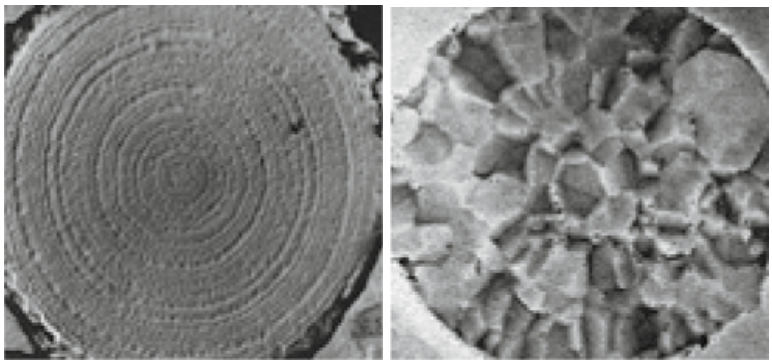

(a) *Onion-skin structure* (b) *Polycrystalline*

Figure 2.9: Onion-skin structure of mechanically hard CIP (a) and polycrystalline structure of mechanically soft CIP (b) (BASF (website), 2010)

2.2.3 Base fluid

The base fluid has the two main objectives of carrying the magnetizable particles and lubricate the MR device. A good base fluid is a non-toxic and non-reactive lubricative liquid with a relatively low viscosity. It should be temperature stable with a high boiling point, low volatility and small variations in viscosity with temperature (high viscosity index). Other important properties of base fluids are low solubility of gases and oxidation resistance. The selection of a base fluid often becomes a compromise between two or more of these properties. Common base fluids are silicone, synthetic, semisynthetic, mineral and lubricating oils but other polar organic liquids and water have also been used as base fluids (Shahinpoor and Schneider, 2008).

For enhanced properties, most commercially used MR fluids also include one or more fluid additive. Surfactant additives decrease the rate of particle settling by lowering the surface tension of the fluid. Long term sedimentation can however not be completely prevented due to the non-colloidal nature of the fluid. Dispersion agents are used to disperse the particles over the fluid volume and reduce agglomeration. Anti-wear or friction reducing additives reduce mechanical friction and scuffing between particles by forming a thin lubricative layer on the particle surface. Antioxidants may be used to prevent oxidation in the fluid. Two or more of these effects may be presented by one additive material. The use of additives may increase or decrease the off-state viscosity of the fluid. Positive effects of an additive on one fluid property may have negative effects on other fluid properties. Choosing additives for a good MR fluid can therefore by tricky.

A former composition of the MR fluid in the prosthetic actuator utilized petroleum based oil as a base fluid. A problem with fluid leakage that was believed to be due to outgassing of the fluid lead to use of a base fluid with lower volatility. The fluid chosen

was a perfluorinated polyether (PFPE) oil (Hsu et al., 2006) of type UNIFLOR^{TM} 8510, produced by Nye lubricants (Nye (2011)). The PFPE base fluid has been shown to have attractive properties, for the proposed application in an MR prosthetic knee, with regards to sedimentation stability and thermal characteristics (Gudmundsson et al., 2011). It behaves like a Newtonian fluid with a viscosity of 0.3 Pa·s that is independent on shear-rate (Gudmundsson et al., 2011) and a relatively high viscosity index.

The current fluid composition also employs a different PFPE oil as a dispersion agent. The oil type is Krytox^{TM} 157-FSL produced by DuPont® (DuPont (2011)) and takes up 5 vol% of the liquid component (Hsu et al., 2006). The density of both base fluid and dispersion agent are relatively high when compared to more common base fluids. The density of UNIFLOR^{TM} 8510 is 1870 kg/m^3 and that of Krytox^{TM} 157-FSL is 1960 kg/m^3. The viscosity of UNIFLOR^{TM} 8510 is relatively high when compared to common base fluids (65 cSt at 40°C) but the lower viscosity of the Krytox^{TM} 157-FSL additive (30 cSt at 40°C) reduces the total off-state viscosity of the fluid. The PFPE base fluid and dispersion agent have relatively good lubricating properties and no specific anti-wear or friction reducing additives are used in the current fluid composition.

2.2.4 Alternative fluid compositions

Currently used fluid composition consists of the PFPE oil mixture described in Section 2.2.3 suspended with 28 vol% of the CIP described in Section 2.2.2. This composition is hereafter referred to as Fluid 1. Analysis of used CIP from the prosthetic actuator reveals spalling of the particle surface and formation of thin flake-shaped particles (see section 4.3). This is believed to cause particle agglomeration and result in IUT. The brittle surface and onion-skin structure of the mechanically hard CIP is believed to play a big role in the effect of spalling. As an attempt to solve this problem, an new MR fluid composition employing mechanically soft particles is tested and compared to the current composition with regard to fluid durability (see Chapter 3). The powder is silica coated mechanically soft CIP of grade CC, produced by BASF. This new fluid composition is hereafter referred to as Fluid 2. Table 1 summarizes important properties of the two powders as specified by the manufacturer. The liquid component and solid concentration in Fluid 1 and 2 are identical.

Table 2.5: Properties of HS and CC CIP as specified by the manufacturer (BASF (2010))

Particles	Mean particle diameter (D50 μm)	Iron content (%)	Mechanically hard or soft
HS (Fluid 1)	2.1	>97.0	Hard
CC (Fluid 2)	6.0	>99.5	Soft

A different attempt was made to solve the problem of particle spalling by using friction reducing additives. A new fluid composition was prepared employing a dithiophosphorus lubricant additive of type Molyvan®L and a dithiocarbamate lubricant additive of type Molyvan®822, both produced by Vanderbilt (2011). The iron powder type and proportion remained unchanged in the new fluid composition. This new fluid composition will hereafter be referred to as Fluid 3. The liquid component of Fluid 1 and Fluid 3 is compared in Table 2.6.

Table 2.6: Liquid component composition of Fluids 1 and 3 (vol%)

Fluid	UNIFLOR^{TM}	Krytox^{TM}	Molyvan®L	Molyvan®822
Fluid 1	95.00	5.00	0.00	0.00
Fluid 3	90.25	4.75	2.50	2.50

The micron-sized gaps in which the fluid is sheared limit the choice of particles. The grade CC particles were chosen due to their size distribution and high iron content. The purpose of the silica coating is to improve powder flow in metal injection molding or powder metallurgy (BASF (website), 2010). Uncoated, reduced CIP with similar size distribution was not found. Stainless steel and water-atomized iron particles have been used in durable fluid compositions. Neither of these particle types were found with size distribution small enough to fit between the steel blades. Cobalt-iron particles exhibit higher magnetic saturation than CIP. These particles may be used to increase the possible braking force if they are durable enough. Different additives such as colloidal graphite could also be employed in future test compositions to decrease mechanical friction and scuffing.

3 Durability tests

3.1 Configuration of tests

The effects of different external factors on the fluid health are tested and compared in Section 3.1.1. To monitor the rate of degradation and compare the durability of different fluid compositions, a test-rig is prepared and durability tests performed. The test rig set-up and characteristics are described in Sections 3.1.2 and 3.1.3, respectively. The procedure of durability tests is described and results presented in Section 3.2.

3.1.1 Pre-investigation

The MR fluid is put to a real challenge in this prosthetic device where different factors such as high temperature and high shear forces can affect the fluid and cause degradation. In search for the main cause of fluid degradation it was decided to split up the different load factors as possible, and test the effect of different load factors on the MR fluid in the device. New knee joint actuators of type Rheo Knee® (Össur hf. (2011)) are assembled, all containing MR fluid from the same mixing batch. Each knee joint was tested to reveal the effect of one specific load factor, although some of the factors overlap.

Cycling the knee joint causes frictional wear on all contact surfaces. Over time it can affect seals and bearings. The fluid could also be affected as it is stirred and flows over the contact surfaces. Frictional wear between other contact surfaces, i.e. steel blades and inner or outer housing can cause tiny fragments of the contact surface material to mix with the fluid. This could affect the rheological properties of the fluid. One actuator was assigned to reveal the effect of mechanical friction and stirring of the fluid without any current applied. The knee joint was cycled to full extension at a rate of 80 cycles per minute. The duration of the test was 95.00 cycles in 20 hours, excluding two pauses due to failure in the cycling device. The outside of the outer knee joint housing reached a steady temperature of 30°C during this test.

High temperatures can accelerate oxidation of particles and/or base fluid. Furthermore, they can contribute to vaporization of the base fluid and outgassing of adsorbed air in the fluid. One actuator was assigned to show the effect of high temperature alone, although actuators in other tests reached high temperatures as well. The actuator was placed in an oven at a controlled temperature of 60°C for 20 hours.

The increase in apparent viscosity in the presence of a magnetic field is partly reversed as the field is turned off and should be completely reversible by the use of degaussing. One actuator was subjected to strong constant magnetic field to see if heavy magnetic build-up over a long time could cause particle agglomeration or in some other way permanently increase the apparent viscosity of the fluid. A power supply was used to generate current of 1.6A through the actuator coil. The voltage was held constant but the current dropped as the temperature rose. The current reached a steady state at 1.3A and the temperature at the outer housing reached as high as 60°C. This was repeated for another actuator but using a square wave instead of a constant current to switch the direction of the magnetic field twice every second. The current amplitude dropped as the temperature rose in the same way as for constant current.

High mechanical forces can cause the iron particles to fracture or deform, as well as causing frictional wear on all contact surfaces and producing heat in the fluid. Testing the effect of this factor in a controlled environment requires setting up a custom test rig and was therefore delayed until after the results from the other tests.

After performing the tests, the actuators were measured for increased stiffness, disassembled, iron particles cleaned from the fluid and the particles and base fluid analysed separately. After analysing and comparing the fluids, a decision was taken to repeat the first test (frictional wear) over a longer period of time. The same test load was applied, but this time for 800.000 cycles in 170 hours.

The colour of the base fluid is light brown after the tests, which indicates minor oxidation of the iron particles. However, oxidation may have occurred while gathering the fluid from the actuator. Particle samples from fluids tested for mechanical friction and stirring show that some particles have fractured. There are clear evidences of surface spalling (see figure 4.5(a)), although majority of the particles appear intact.

It is concluded that high temperature or current alone have negligible effect on the fluid in the device over a short period of time, and the effect of mechanical friction has a very limited effect. Shear forces are believed to be the main mechanism responsible for the degradation of the fluid. The test rig was improved so that it could cycle the knee while current was lead through the coil, subjecting the fluid to high shear forces.

3.1.2 Test rig set-up

User tests have shown that a fast and steep downhill walk can result in noticeably increased stiffness of the knee-joint over a very short period of time. From that knowledge and the results from previous tests in section 3.1.1, a hypothesis was made that the primary cause of the fluid degradation is spalling of the iron particles as the fluid is subjected to high shear stresses. A test rig was set up to repeatedly build up the chains of particles in the fluid and break them down. The goal was to reach the highest shear stresses that can occur in real-world usage, that is when the amputee is walking down stairs. The test rig is simple and inexpensive and is not meant to accurately simulate walking. However, it does subject the fluid to repeated high shear stresses, similar as in down-hill or down-stairs walk.

An electric motor cycles the knee joint between 29 and 69° angle from upright position, 100 cycles per minute. Maximum possible angle is 122° from upright position. The reason for the fast pace and limited angle range is to reduce the required test duration and motor size, respectively. The current is switched on when the angle from upright position is decreasing and reaches 35°. Current is switched off again when the angle reaches 50°. Current is not switched on when the angle is increasing, so there is only one current spike per cycle. The angle interval was chosen where the torque output of the device was at its maximum to minimize the size of motor required. The current reaches above 1.5A in every cycle (see figure 3.1(a)).

On-state torque, off-state torque and swing-extension are measured several times during the test with an increasing interval. A microcomputer in the knee switches the current direction every other step to prevent magnetization build-up in the actuator. However, there can be a small difference between the current duration and/or amplitude in positive and negative direction. Therefore some magnetization builds up with time, making the actuator noticeably stiffer. The actuator is therefore degaussed before every measurement. Cycling the actuator afterwards without applying current turned out to be necessary for the degaussing to work effectively. After the actuator is cycled 1000 times to full extension with no current applied it is stored at room temperature for 2 hours to reach ambient temperature before measurements.

3.1.3 Test rig characteristics

Figures 3.1(a) and 3.1(b) show measured coil current and knee joint angle as a function of time during the durability test. Current through one cycle varies with users and different walking styles. Figure 3.1(c) shows the mechanical torque, generated by the actuator, as

a function of time. The torque curve is derived from measured current and the current-torque relation in figure 2.4. Figure 3.1(d) shows the mechanical power generated in the actuator, as a function of time. The mechanical power is the product of mechanical torque and angular speed.

Values for current, angular speed, torque and power are summarized in Table 3.1. The duration of one test-cycle is 0.59s which is 50% shorter than that for walking on level ground. The highest current amplitude is almost as high as for walking down stairs but the mean current is much lower. LDE of an MR fluid in the durability test is $9.3 \cdot 10^6 J/cm^3$ per $10^6 cycles$. This is 50% higher than for walking on level ground but 72% lower than for walking down stairs. The short duration of each test-cycle and high dissipation of energy reduces the period of time required for each test. This was necessary to finish the durability tests within the time frame of this project. To reach the durability threshold of $10^7 J/cm^3$ the knee joints must be tested for $1.1 \cdot 10^6$ cycles.

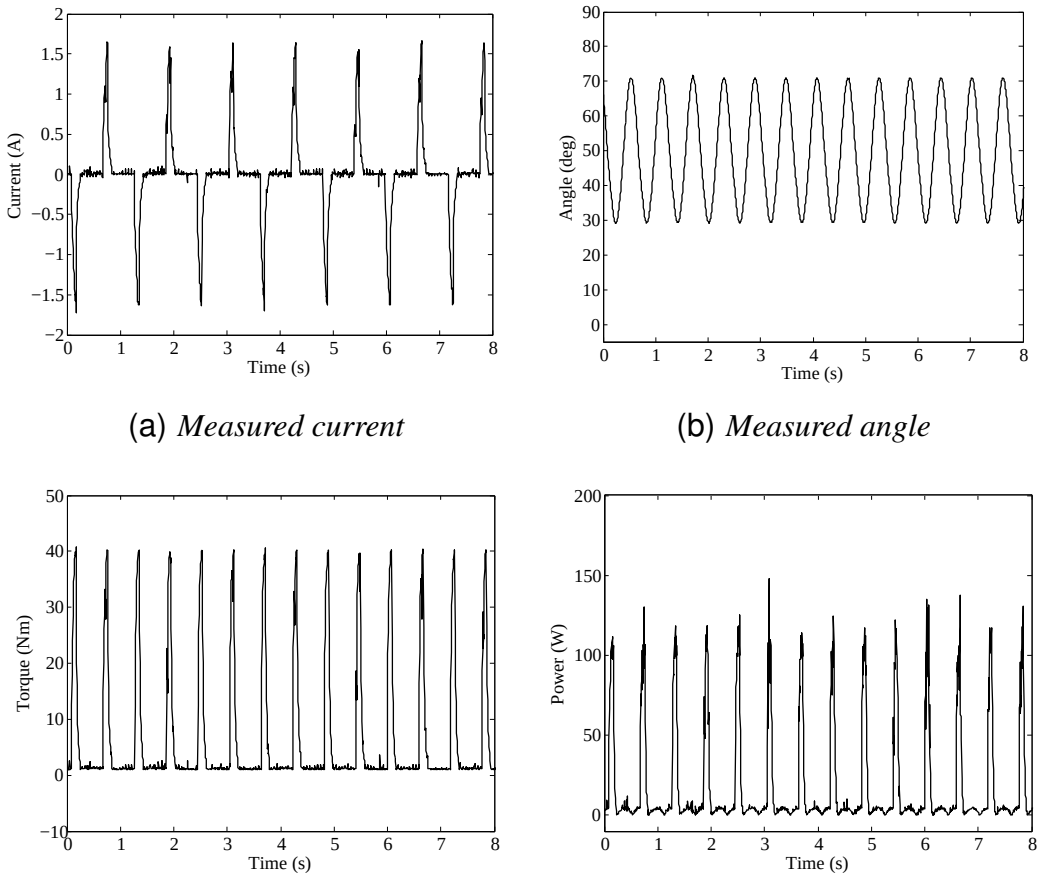

(a) *Measured current* (b) *Measured angle*

(c) *Calculated torque* (d) *Calculated power*

Figure 3.1: Characteristics of the test rig

Table 3.1: Summary of characteristic values for the test-rig

	Current	Angular speed	Torque	Power
Max	1.7 A	6.7 rad/s	40.7 Nm	147.7 W
Mean	0.2 A	2.5 rad/s	6.7 Nm	17.8 W
RMS	0.5 A	2.7 rad/s	13.4 Nm	37.3 W

3.2 Procedure and results

This section describes measurements performed on Rheo Knee® (Össur hf. (2011)) actuators during the durability tests described in Section 3.1. Mechanical wear of the actuator components is discussed in Section 3.2.1. Off- and on-state torque of the actuators is monitored and presented in Sections 3.2.2 and 3.2.3, respectively. The turn-up ratio of each fluid before and after the test is evaluated from the results and presented in Section 3.3.

3.2.1 Mechanical wear

Mechanical scuffing between the steel blades and inner- and outer housing can cause the contacting parts to wear and decrease the rigidness of the joint. The mechanical wear criteria for used knee joints in service is that angular play is less than 2.5°. This was not monitored in the durability test in the same way as on- and off-state torque. The actuator play was measured 1.4° for actuator containing Fluid 1 after $1.5 \cdot 10^6$ cycles. There was not a measurable play in actuators containing Fluid 2 and 3, which is believed to be due to the high stiffness.
The blades are made of steel, the inner housing of titanium and the outer housing of nickel-coated aluminium. The main reason for the increased play is believed to be the steel blades grinding down the aluminium outer housing. This results in increased aluminium and nickel in the fluids as measured in Section 4.4.

3.2.2 Off-state torque

Cycling the knee was paused a number of times with an increasing interval to measure the on-state torque, off-state torque and swig extension of the knee joint. Actuator containing Fluid 1 was tested to $2.5 \cdot 10^6$ cycles but tests on Fluids 2 and 3 were stopped after 10^6 cycles when it was clear that they exhibited poorer durability than Fluid 1.

Actuator stiffness can be evaluated by measuring the swing extension, which is directly

proportional to the off-state torque. The swing-extension is measured using a custom device. A weight is attached to the lower part of the knee to simulate the weight of the leg and foot. The actuator is manually cycled 50 times to warm it up. The weight is then pulled backwards to a certain angle and dropped and the swing extension is read off a digital spirit level.

Figures 3.2(a) - 3.2(c) show how the swing extension decreases with number of cycles. Despite high fluctuations in measured values, there is a clear downwards trend in the swing extension for all three actuators. The actuators are stored at room temperature ranging from 22 to 24°C for at least two hours before each measurement to reach ambient temperature. Variation in storage time before each measurement is believed to be the main reason for the fluctuation in measured values. Storing the actuator for too long increases the effect of particle settling and increases the off-state torque. The first three measurements on the knee joint with Fluid 1 are excluded because the actuator was not cycled between degaussing and measuring, which turned out to be necessary to remove the effect of magnetic build-up.

The swing extension criteria for new production knees is angular travel $> 39^\circ$ and for used knees in service is $> 32^\circ$. For actuator with Fluid 1, all measurements after $5 \cdot 10^5$ cycles fail the criteria for service knees. The same applies for Fluid 2 after $1 \cdot 10^5$ cycles and Fluid 3 after $6 \cdot 10^5$ cycles.
For Fluid 1 the swing extension seems to decrease at a linear rate as a function of test-cycles. The rate of decrease is approximately 0.5° per 10^5 cycles ($R^2 = 0.79$). For fluid 2 the swing extension drops to zero after less than 10^5 cycles. Swing extension for Fluid 3 decreases by approximately 0.5° per 10^5 cycles ($R^2 = 0.96$) but suddenly drops to zero after more than $7 \cdot 10^5$ cycles.

The off-state torque was also measured directly using a simple dial torque meter. The knee joint was turned from 0 to 90° at approximately $\pi/4$ rad/s and the final value read off the dial. Due to low values of off-state torque and manually controlled angular speed, the accuracy is low. The results are plotted in Figures 3.3(a) - 3.3(c). Note the different scales on vertical axis. The rate of increased torque for Fluid 1 is 0.024Nm per 10^5 cycles with a coefficient of determination of 0.73. For Fluid 2 the initial off-state torque is low but quickly increases above acceptable values, and reaches as high as 13Nm. Due to high fluctuations in measured torque, a straight line does not fit well to the data points for Fluid 2. Fluid 3 shows no measurable increase in off-state torque until after more than $7 \cdot 10^5$ cycles when it starts to increase at a very high rate. This is in agreement with the swing extension measurements.

A spring that pulls the knee joint to an upright position when brake is released was not removed before each of the periodical experiments since it is glued to the actuator. The spring therefore affects the measurements by increasing the measured torque. However,

the off-state torque of the actuators was measured before attaching the spring and after detaching it after 10^6 cycles. For actuator containing Fluid 1 the test was extended to $2.5 \cdot 10^6$ cycles before detaching the spring again and measuring. The results are listed in Table 3.2. Equation 2.2 is used to calculate the corresponding viscosity of the MR fluid. For Fluid 1 the off-state torque increases by more than 100% over the first 10^6 cycles but surprisingly does not increase over the next 10^6 cycles. The last measurement is inconsistent with the previous measurements and is considered faulty.

Table 3.2: Off-state torque of actuator T_{off} without spring attached and corresponding fluid viscosity μ.

Fluid \ cycles	0	$1.0 \cdot 10^6$	$2.5 \cdot 10^6$
Fluid 1 - T_{off}	1.0 Nm	2.2 Nm	(2.1 Nm)
Fluid 2 - T_{off}	1.2 Nm	11.0 Nm	-
Fluid 3 - T_{off}	1.1 Nm	14.0 Nm	-
Fluid 1 - μ	1.3 Pa s	3.9 Pa s	(3.6 Pa s)
Fluid 2 - μ	1.7 Pa s	22.7 Pa s	-
Fluid 3 - μ	1.5 Pa s	29.2 Pa s	-

A third method to evaluate the actuator stiffness is to cycle the knee joint with the lower end fixed and measuring the output of load cells in the knee. This is a relatively accurate method to compare actuators since an electric motor rotates the knee joint while a computer reads the output of the load cells. However, there is no easy way of converting the load cell output to actuator torque in Newton-meters. The device returns a unitless value derived from the output signals of two load cells. The knee joints stiffness was measured using this method before and after the durability tests, and after 10^6 cycles for actuator with Fluid 1. Results are listed in Table 3.3. The stiffness of actuator containing Fluid 1 increases by the same value over the first 10^6 cycles as over the next $2.5 \cdot 10^6$ cycles, indicating that the rate of stiffening is close to linear. The stiffness of actuators containing Fluid 2 and 3 was too high after the durability test for the electric motor to cycle it, and could therefore not be measured. The criteria for new actuators is device output < 23.

Table 3.3: Unitless values derived from the output of load cells in the knee. Measured in off-state mode.

	Fluid 1	**Fluid 2**	**Fluid 3**
0	19	20	20
10^6	25	Too stiff	Too stiff
$2.5 \cdot 10^6$	31	-	-

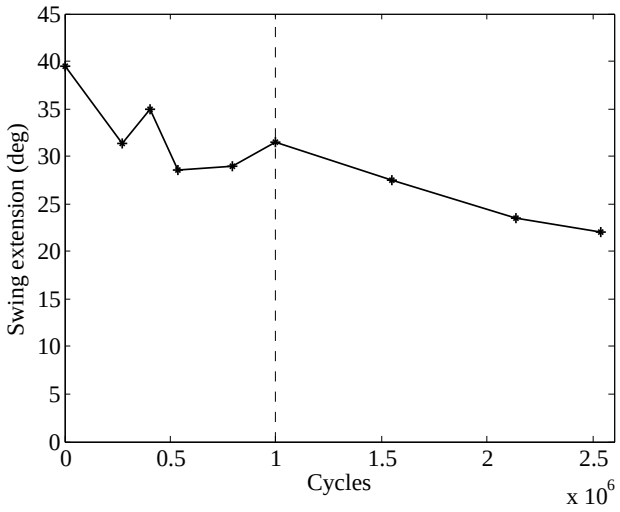

(a) *Actuator with Fluid 1*

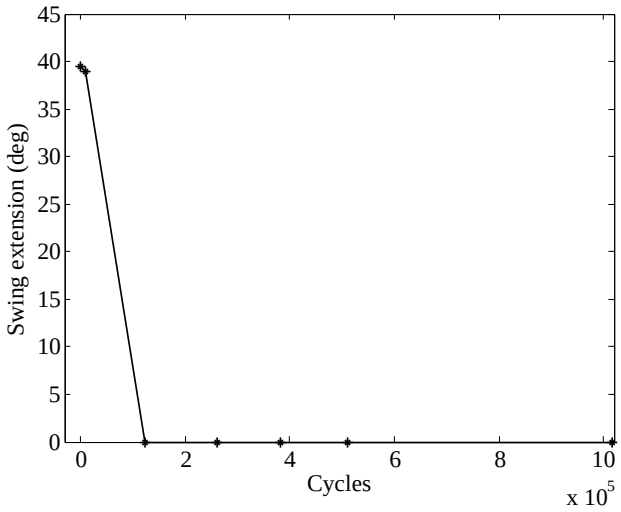

(b) *Actuator with Fluid 2*

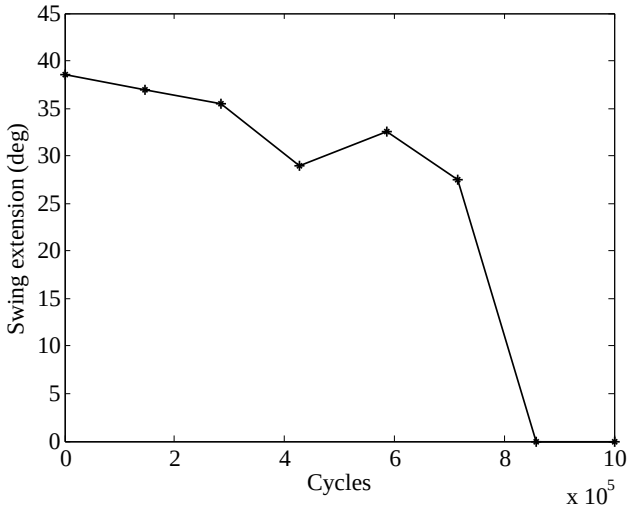

(c) *Actuator with Fluid 3*

Figure 3.2: Measured swing extension of knee joint as a function of test cycles

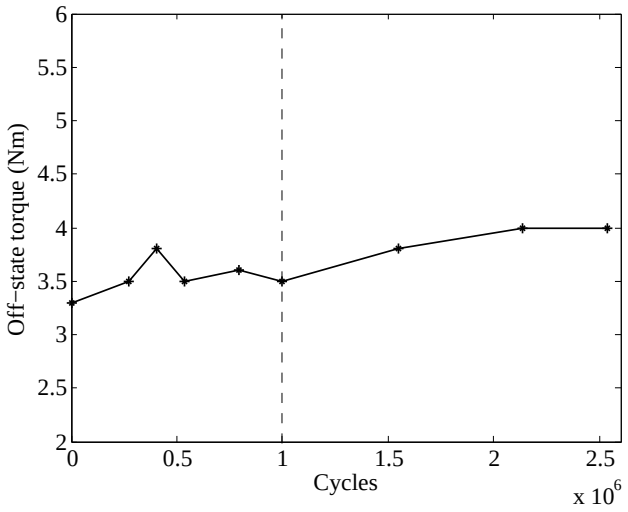

(a) *Actuator with Fluid 1*

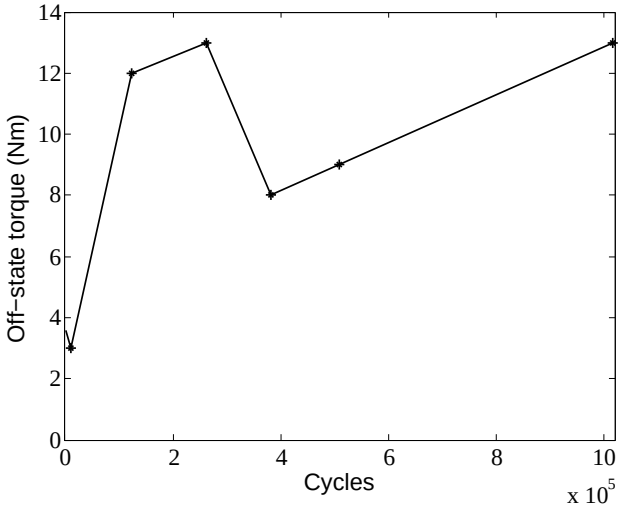

(b) *Actuator with Fluid 2*

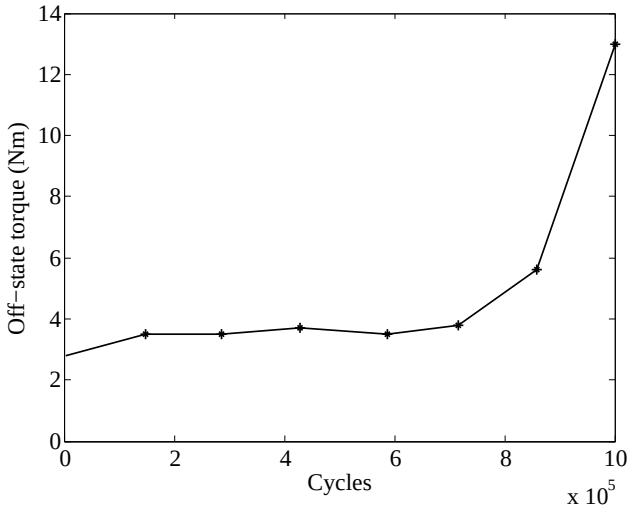

(c) *Actuator with Fluid 3*

Figure 3.3: Measured off-state torque as a function of test cycles

3.2.3 On-state torque

The actuator torque was measured in on-state mode as well as off-state. The torque was measured at a constant 1.5A coil current using a simple dial torque meter. The torque at yield point was obtained by slowly turning the torque meter from upright knee position and reading the value just before slip occurs. A second value was also read at 45° angle. Note that spring is attached to the actuator during these measurements.

Figures 3.4(a) - 3.4(c) show how the measured torque changes with number of cycles for actuators containing fluids 1-3. The first three measurements are excluded due to magnetic build-up as explained in previous section. For actuator containing Fluid 1 the on-state torque decreases at a rate of approximately 0.4Nm per 10^5 cycles (coefficient of determination is $R^2 = 0.92$). Despite high fluctuations there is a clear downwards trend and the decrease is not far from linear. The torque suddenly increases again in the last measurement after $2.5 \cdot 10^6$ cycles. The reason for that is unknown.
On-state torque of actuator containing Fluid 2 decreases by 4Nm in the very beginning of the test. The average rate of decrease is 2.5Nm per 10^5 cycles over the first $5 \cdot 10^5$ cycles but the decrease is much slower after that.
The on-state torque at yielding for actuator containing Fluid 3 is low from the start and does not decrease much. It increases in the last measurements, probably as a result of highly increased off-state torque.
The on-state torque at yield point for unused actuators containing Fluids 1 and 2 returned similar values which is unexpected noting that Fluid 2 has purer iron particles.

The on-state torque of the knee joints was also measured before attaching the spring and after removing it after 10^6 cycles. For actuator containing Fluid 1 the test was continued and the on-state torque measured again without spring after $2.5 \cdot 10^6$ cycles. The results are shown in Table 3.4. Equation 2.4 is used to calculate the corresponding shear stress in the MR fluid. The results are in harmony with the periodic measurements with a spring attached. The absence of spring simply offsets the torque downwards.

Table 3.4: On-state torque of actuator T_{on} without spring attached and corresponding shear yield stress σ_y

Fluid \ cycles	0	$1.0 \cdot 10^6$	$2.5 \cdot 10^6$
Fluid 1 - T_{on}	36 Nm	30 Nm	30 Nm
Fluid 2 - T_{on}	34 Nm	24 Nm	-
Fluid 3 - T_{on}	32 Nm	35 Nm	-
Fluid 1 - σ_y	38 kPa	32 kPa	32 kPa
Fluid 2 - σ_y	36 kPa	26 kPa	-
Fluid 3 - σ_y	34 kPa	37 kPa	-

As for off-state torque in the previous section, the knee joint braking torque was evaluated from load cell output when cycling the knee joint in a custom built device. The load cell output was measured for the actuators with no spring attached before the test, after 10^6 cycles and also after $2.5 \cdot 10^6$ cycles for actuator containing Fluid 1. However, the stiffness of actuators containing Fluid 2 and 3 was too high after the durability test for the electric motor to cycle it. Results are presented in Table 3.5. The load cell output criteria for new knees is device output >460.

Table 3.5: Unitless values derived from the output of load cells in the knee. Measured at 1.5A coil current

Cycles	**Fluid 1**	**Fluid 2**	**Fluid 3**
0	495	525	481
10^6	427	Too stiff	Too stiff
$2.5 \cdot 10^6$	430	-	-

Here the measured on-state torque of unused actuators is noticeably highest for Fluid 2. It is concluded that a small shear-rate is required to reveal the superior magnetic properties of the purer iron particles. However, the higher iron content also reduces the mechanical strength of the particles which is believed to cause the highly increased off-state torque. The measured output for fluid 1 decreases by 14% over the first 10^6 cycles and reaches far below the minimum criteria for used knees. However, there is almost no total change over the next 10^6 cycles due to a sudden torque increase at the end of the test.

3.3 Turn-up ratio

Turn-up ratio is defined as the ratio of on-state shear yield stress to off-state viscosity. It is used to evaluate the overall MR performance of the fluid. The turn-up ratio for the three fluids before and after durability tests are listed in Table 3.6. Fluid 1 exhibits the highest initial value and also the lowest decrease in turn-up ratio. It is therefore considered the best and most durable of these three fluids.

Table 3.6: Turn-up ratio

Cycles	**Fluid 1**	**Fluid 2**	**Fluid 3**
0	$3.6 \cdot 10^4\, s^{-1}$	$2.8 \cdot 10^4\, s^{-1}$	$2.9 \cdot 10^4\, s^{-1}$
10^6	$1.3 \cdot 10^4\, s^{-1}$	$2.2 \cdot 10^3\, s^{-1}$	$2.5 \cdot 10^3\, s^{-1}$
Decrease	62%	92%	91%

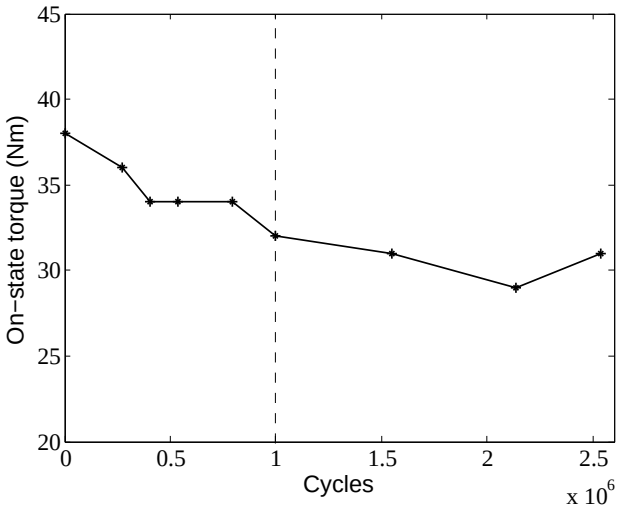

(a) *Actuator with Fluid 1*

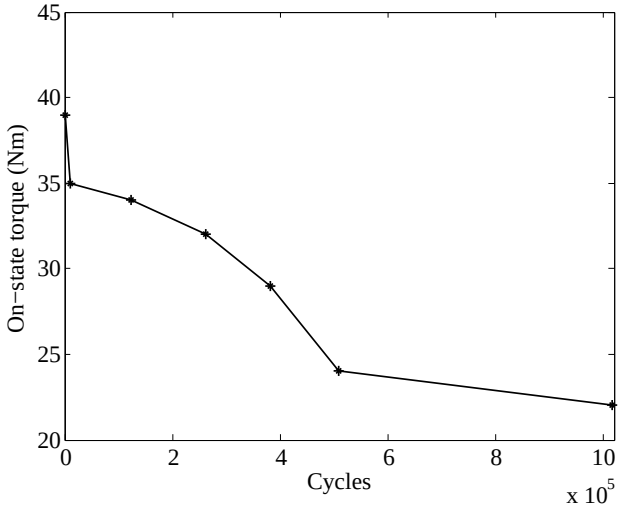

(b) *Actuator with Fluid 2*

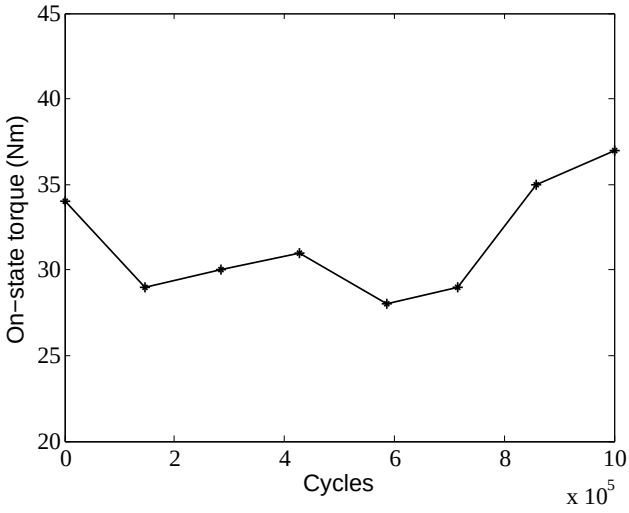

(c) *Actuator with Fluid 3*

Figure 3.4: Torque at yield point for 1.5A coil current

4 MR fluid analysis

Measurements performed on used and unused MR fluids are described and the results compared. MR fluids are measured after an actual usage by an amputee or after excitation in a test rig. Measurements are performed in Iceland at Össur hf. (2011) and Innovation Center Iceland (Innovation Center Iceland (2011)). When necessary equipment is not available in Iceland, measurements are performed in Brazil in cooperation with Prof. Antonio Bombard at the Itajubá Federal University (UNIFEI (2011)). Section 4.1 describes a method developed to prepare used MR fluids for measurements and analysis. Section 4.2 describes the visual appearance of the fluid as it is adapted from the actuators. The morphology of used and unused particles is analysed and described in Section 4.3. Section 4.4 describes the measured chemical composition of particles and base fluids. Samples are sent abroad for particle size distribution and magnetization measurements. The results are presented in Sections 4.5 and 4.6, respectively.

4.1 Fluid prepared for measurements

The actuators are disassembled and the used MR fluid collected. The fluid appears as a sticky layer on the steel blades and other contact surfaces. The fluid is cleaned off the blades and other parts, one at a time, using a solvent. The solvent is a hydrofluorocarbon fluid of type Vertrel XF^{TM}, produced by DuPont® (DuPont (2011)). With the diluted MR fluid in a glass bottle, a strong constant magnet is used to attract the particles to the bottom of the bottle (see Figure 4.1). The oil and solvent mixture is then poured off and clean solvent poured in the bottle. The particles are stirred in the solvent to clean off any last oil and the magnet used again to pour the oily solvent off. The particles are then stored in clean solvent to prevent oxidation or caking. Both the particles and oil-solvent mixture are preserved for measurements. The total amount of solvent used is approximately 10 times the amount of MR fluid.
Due to the high volatility of the solvent, preparing dry iron particles for measurements and analysis is simple. The solvent with particles is poured onto a sample holder and the sample is ready when all the solvent has evaporated. To analyse the structure of the powder under the influence of a magnetic field, a solvent with particles is poured onto a sample holder with carbon glue while holding a constant magnet under the sample holder. The particles line up in the magnetic field in the solvent and stick to the carbon glue when the solvent evaporates. The results are shown in Section 4.3.

Figure 4.1: Extraction of CIP from base fluid using solvent and a magnet

4.2 Visual inspection

Unused MR fluids of type 1, 2 and 3 all look alike. There is not a noticeable difference in Fluid 1 appearance before and after the durability test (see Figure 4.2(a)). Fluid 2 appears as a thick, black paste after the durability test (not shown in Figure). Fluid 3 has dried up during the test (see Figure 4.2(b)). Similar dried fluid has also been noticed in old, heavily used knee joints with Fluid 1.
New fluid has a gray colour since it consists of gray iron particles and colourless or nearly colourless fluids. The additives in Fluid 3 give the liquid component of the fluid a light red/brown colour (see diluted in solvent in Figure 4.3(b)). The liquid component of the fluids becomes very dark during the durability tests or actual usage, darker than the original fluid including iron powder (see Figure 4.3(a)). This applies to all the compositions tested.

Unused base fluid is colourless. After removing the particles from MR fluids that have been tested for a few cycles or heat aged in prosthetic actuators, the base fluid shows a light brown colour. This indicates light oxidation of the iron particles. Some oxidation may however have occurred during the cleaning procedure described in Section 4.1. Base fluids from longer durability test have a dark gray colour, and base fluids after many months of real-world usage are black. Figure 4.3 shows an unused MR fluid and base fluids before and after durability tests. Nano-sized iron powder and/or oxidised nickel from the outer housing of the fluid chamber is considered most likely to have caused the dark colour. Due to the chemical composition of the PFPE oil it is considered unlikely that the oil itself has oxidized. Also, the iron particles should work as an oxidation inhibitor for the PFPE oil since they have much greater tendency to oxidise.

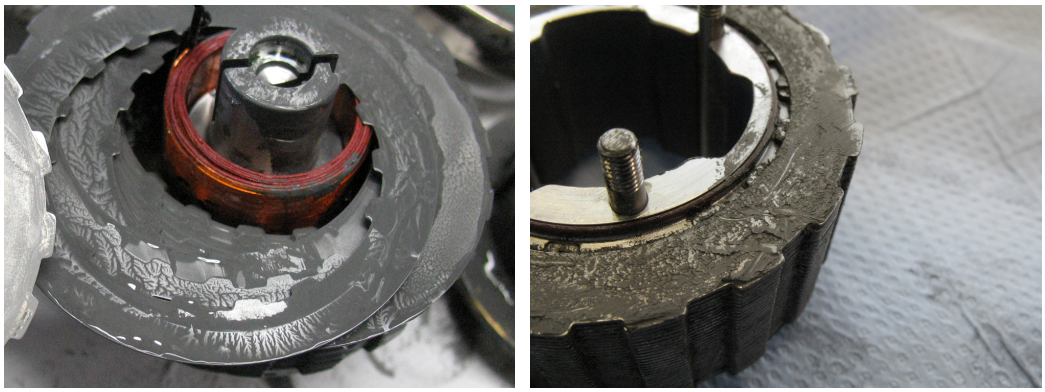

(a) *Fluid 1* (b) *Fluid 3*

Figure 4.2: Fluid 1 (to the left) looks unchanged after the test but Fluid 3 (to the right) has dried up

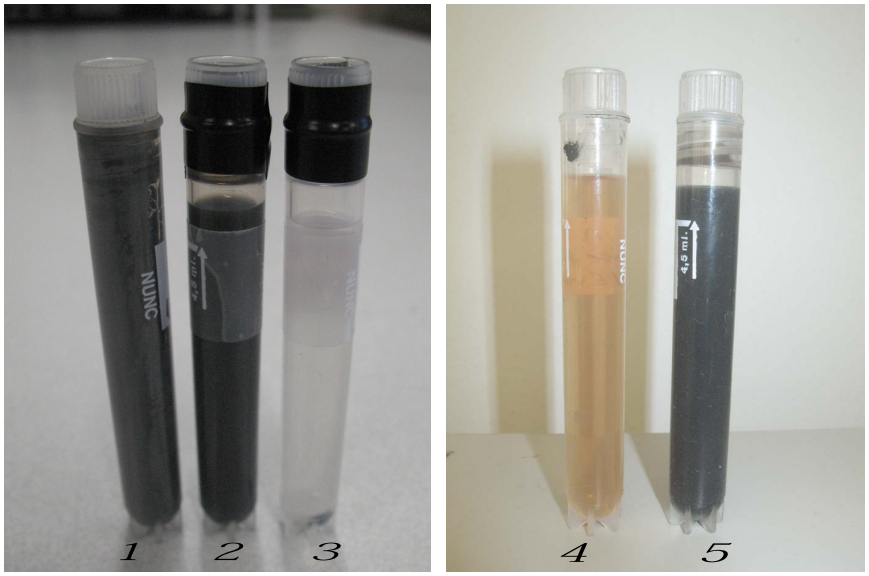

(a) *Fluid 1* (b) *Fluid 3*

Figure 4.3: (1) Unused Fluid 1 (2) Base fluid 1 after $2.5 \cdot 10^6$ *test cycles*
(3) Unused Base fluid 1 (4) Unused Base fluid 3 (5) Base fluid 3 after 10^6 *test cycles*

4.3 Particle morphology

A Scanning Electron Microscope (SEM) is used to analyse the morphology of used and unused particles. The SEM type is Leo Supra 25 and it is located at Innovation Center Iceland (Innovation Center Iceland (2011)). It was operated by professionals at the Innovation Center by the request and at the presence of the author.

Images of unused CIP of grade HS (see Figure 4.4(a)) show spherical particles with a smooth and clean surface. The largest particles found are approximately $3\mu m$ in diameter and the smallest ones are approximately $200nm$. Majority of the particles are between 0.5 and 2.0 μm. The only fault observed in the unused powder is multiple spheres stuck in together forming one particle. The largest particles are commonly formed of two spheres but the smallest ones form long wires of numerous iron spheres in some cases. This is believed to be a fault in the production process of the carbonyl iron powder.
CIP of same grade are analysed after an actual usage in an MR fluid in a prosthetic knee actuator. The powders are extracted from MR fluid samples from six different used actuators. The actuators vary in age and registered number of cycles as well as off- and on-state performance.
Some actuators exhibit high stiffness after a few months of little usage (few steps). The CIP from these actuators appears similar to unused CIP, although a few fractured particles are noticed (see Figure 4.4(b)). The reason for the degradation of these actuators is believed to be particle sedimentation due to little movement of the fluid over a long period of time.
CIP adapted from stiff actuators after more than 10^5 cycles of usage contains a mass of flake-shaped particles. Figure 4.4(c) shows an SEM image of CIP after $4.7 \cdot 10^5$ cycles of real-world usage over 2.5 years and Figure 4.4(d) after $7.2 \cdot 10^5$ cycles of usage over 2.5 years. Both actuators were very stiff and fulfilled neither off-state nor on-state torque criteria. Majority of the flakes have a maximum diameter ranging from 0.2 to 2 μm and thickness of a few nanometers. The amount of flakes appears to increase with stiffer, older and more used actuators. These flakes are believed to originate from the particle surface. When two particles of mechanically hard and brittle material collide due to shear forces, the surface fractures and spalls. The onion-skin structure of the mechanically hard CIP is believed to play a big role in this effect. Larger fragments of spheres are also observed, where particles appear to have broken in two or few pieces.

Different flakes are found when the used PFPE base fluid is analysed after the extraction of the CIP. The PFPE oil is diluted with many times its volume of solvent, poured onto a sample holder and let evaporate at room temperature. These flakes are distinctive in size, shape and shade. Elemental analysis in Section 4.4 indicates that these flakes originate from the inner- and outer housing of the fluid chamber. Due to their non-ferromagnetic material, most of these flakes are left in the oil when when a magnet is used to extract the CIP. Flakes of nickel and titanium from the base fluid are shown in Figure 4.5(b).

Using a method described in Section 4.1, the structure of particles formed in a magnetic field can be analysed. Figures 4.7(a) and 4.7(b) show how used CIP grade HS forms long columns. This is in agreement with Cutillas et al. (1998) and Flores et al. (1999) who observed columns or cylindrical structures of particles in MR fluids rather than chains or lattice structure. The columns are 10-20μm in diameter after having flattened out on the sample holder surface. Flakes and fractured particles are included in the column. Note however that this structure was formed in a low viscosity solvent and might therefore vary from the structures formed in the high viscosity base fluid and dispersion agent.

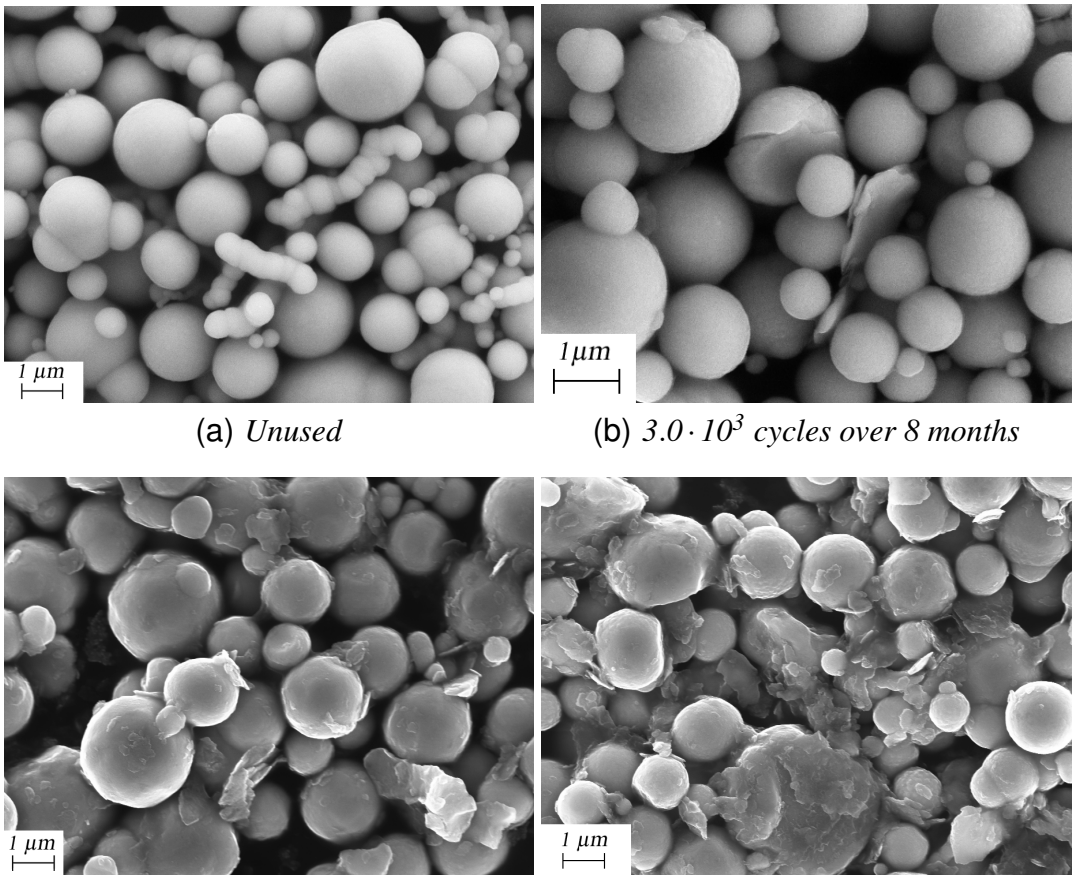

(a) *Unused* (b) $3.0 \cdot 10^3$ *cycles over 8 months*

(c) $4.7 \cdot 10^5$ *cycles over 1.5 years* (d) $7.2 \cdot 10^5$ *cycles over 2.5 years*

Figure 4.4: CIP grade HS after real-world usage

The test actuators from the pre-investigation in Section 3.1.1 are disassembled and the fluid collected. The CIP is extracted and prepared for SEM analysis. The particles appear mainly intact. There is no apparent change in morphology for particles tested for high temperatures or magnetic build-up. Particles from actuators subjected to mechanical friction show evidences that the particles surface is beginning to fracture and spall (see Figure 4.5(a)). However, majority of the particles appear intact.

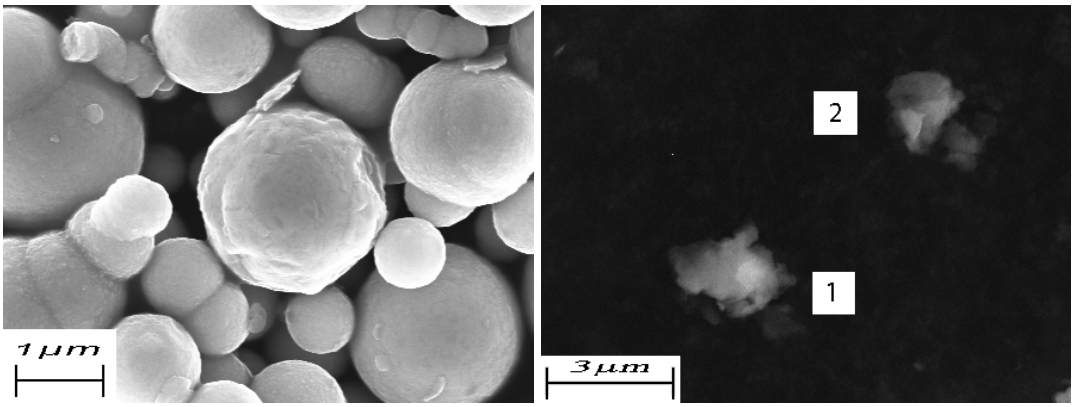

(a) *Surface spalling* (b) *Flakes of nickel and titanium*

Figure 4.5: (a) Particle surface spalling (b) Flakes from base fluid consisting mainly of (1) nickel (2) nickel and titanium

Samples of CIP from the same batch are analysed before and after the durability test described in Chapter 3. CIP extracted from Fluid 1 before and after a durability test are shown in Figures 4.6(a) and 4.6(b), respectively. The used powder contains flakes and fractured and deformed particles but not on the same scale as powders from real-world usage (see Figure 4.4).
CIP of grade CC extracted from Fluid 2 before and after a durability test is shown in Figures 4.6(c) and 4.6(d), respectively. The size distribution for unused CIP grade CC appears broader than for grade HS and with a larger mean diameter. The smallest particles appear of similar size to the smallest particles in the grade HS powder but the largest particles have an irregular shape with the largest diameter up to $8\mu m$. During the test the powder has transformed to a paste and individual spherical particles are not found. It is concluded that the ductile particles of reduced CIP cannot withstand the shear forces generated in the knee joint actuator. The silica coating on the grade CC particles may be partly responsible for the paste shown in Figure 4.6(d).
Grade HS particles extracted from Fluid 3 before and after the test are shown in Figures 4.6(e) and 4.6(f), respectively. Fractured particles and thin flakes are observed in the used powder. The particles appear more damaged than those extracted from Fluid 1 (Figure 4.6(b)) but less damaged than particles after real-world usage (Figure 4.4).

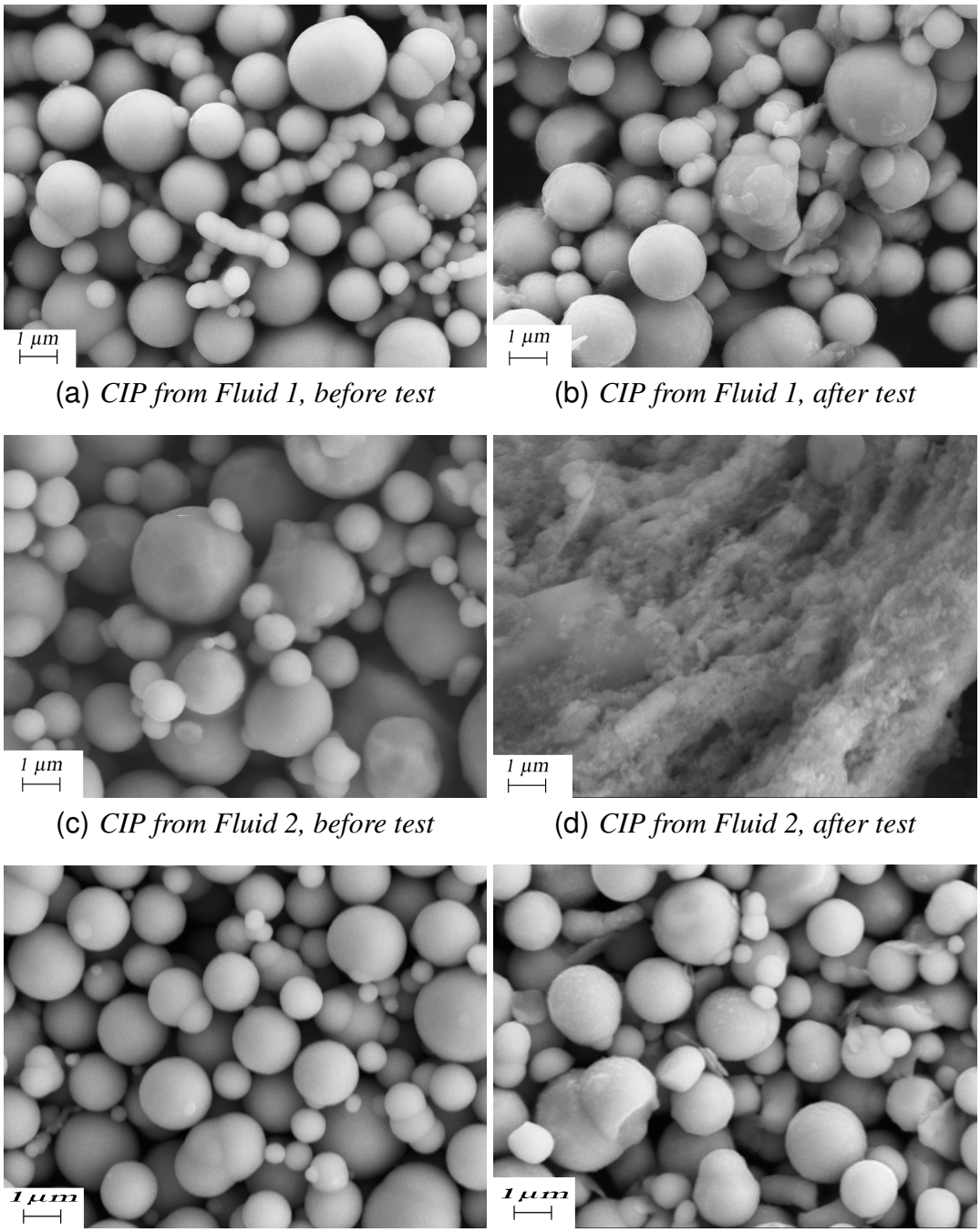

(a) *CIP from Fluid 1, before test* (b) *CIP from Fluid 1, after test*

(c) *CIP from Fluid 2, before test* (d) *CIP from Fluid 2, after test*

(e) *CIP from Fluid 3, before test* (f) *CIP from Fluid 3, after test*

Figure 4.6: Particles before and after durability test

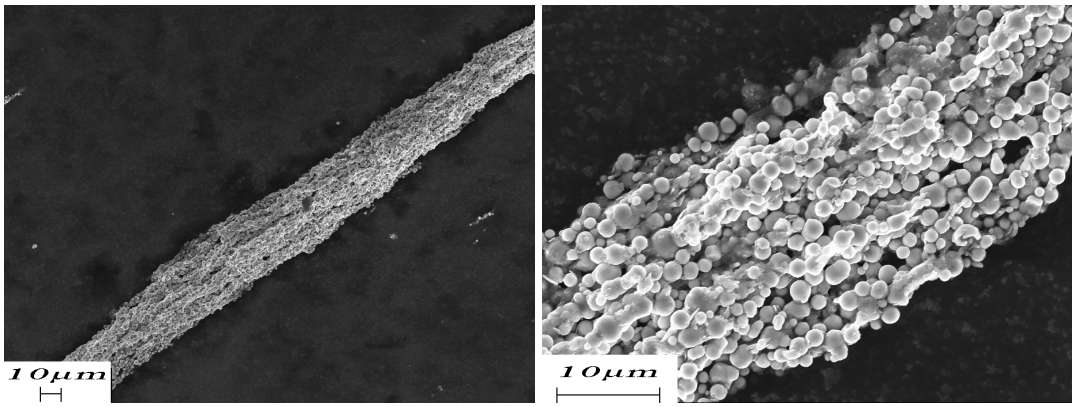

(a) *Overview* (b) *Close-up*

Figure 4.7: Column of used particles, formed in a magnetic field

4.4 Elemental composition

The chemical compositions is analysed for used MR fluids and compared to that of unused fluids. The elemental composition of unused and used base fluids is analysed using Inductively Coupled Plasma Optical Emission Spectrometry (ICP-OES). The measurements are carried out by professional staff at Innovation Center Iceland(Innovation Center Iceland (2011)). The chemical compositions of unused and used iron particles are measured using Energy-Dispersive X-ray Spectroscopy (EDS), connected to the SEM described in Section 4.3.

New CIP that has never been mixed into a fluid shows only iron and carbon. The carbon content is measured 5-7wt% at the particle surface. Particles extracted from unused MR fluid additionally show around 0.5wt% oxygen, possibly due to oxidation in the cleaning procedure. Oxygen content in used particles is not perceptibly higher than that of unused particles. There is not a measurable difference in elemental composition between the spherical particles and deformed or fractured ones from the used fluids. The thin flakes from the particle surface also exhibits the same composition as the primary particles. There are however different flakes that show high contents of aluminium, nickel and titanium (see figure 4.5(b)). These flakes originate from the building blocks of the fluid chamber, the inner part consisting of titanium and the outer part of nickel-coated aluminium. The carbon and oxygen content may be highly over-estimated in all measurements since the sample background, which is approximately 85wt% carbon and 10wt% oxygen, can affect the measurement. This should have the same effect on all the powders measured.

Ulicny et al. (2007a) measured the thickness of the oxide layer on used particles by mixing them into epoxy, cross-sectioning and polishing. By preparing the particles this way it is possible to measure the elemental composition through the cross-section of the particles. Used CIP of grade HS was prepared using this method. The epoxy is non-conductive and therefore needs to be coated with carbon or gold before measuring. Figure 4.8(a) shows a piece of gold-coated epoxy containing used CIP grade HS. Figure 4.8(b) is an SEM micrograph of a cross-sectioned particle at the polished surface. The oxygen content showed to be almost constant over the cross-section. Carbon content was measured highest at the surface and lowest in the center of the particle, which is believed to be due to carbon measured in the epoxy.

Comparing elemental composition at the surface on used and unused particles and measuring the elemental composition through the cross-section of a used particle shows that particle oxidation has not occurred at a measurable degree.

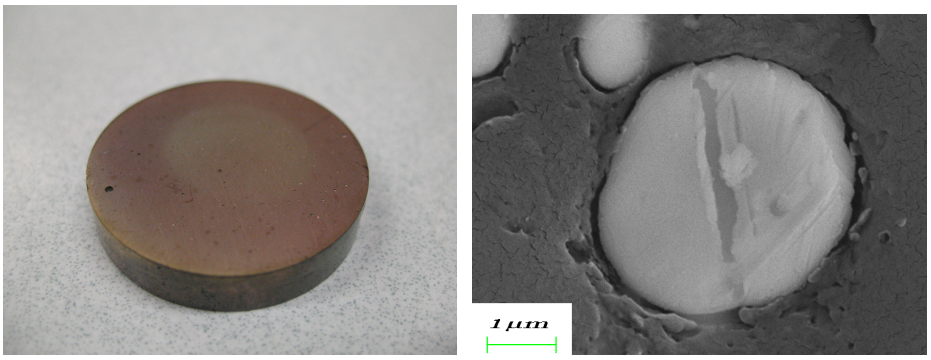

(a) *Epoxy containing CIP* (b) *Cross-sectioned particle*

Figure 4.8: Cross-sectioned CIP for elemental analysis

The amount of metallic elements is measured in used and unused base fluids using ICP-OES. Results are shown in Table 4.1. Only slight traces of iron are found in the unused fluid but used fluid contains 185 ppm of iron. The used fluid additionally contains traces of aluminium, silica, nickel, titanium, zinc and manganese in magnitudes below 50 ppm. All of these elements are found in the building blocks of the actuator. Traces of metals or metal-oxides are believed to be responsible for the dark colour of the used base fluids.

Table 4.1: Metals and metalloid measured in used and unused base fluids

	Fe ppm	**Al** ppm	**Si** ppm	**Ni** ppm	**Ti** ppm	**Zn** ppm	**Mn** ppm
Unused base fluid	2.9	-	-	-	-	-	-
Used base fluid	185	50	26	16	6.9	3.3	0.64

4.5 Particle size distribution

The particle size distribution (PSD) of unused CIP of grades HS and CC was measured using a Low Angle Laser Light Scattering (LALLS) device. The measurements were carried out in a laboratory in Brazil under the supervision of Prof. Antonio Bombard (UNIFEI (2011)). Figure 4.9 shows the volume based PSD for both grades, which is calculated initially from measured data and returned by the LALLS instrument. The number based PSD is derived from the volume based PSD and shown in Figure 4.9.

The HS powder exhibits a broad size distribution with a peak at approximately 1.5μm. The size distribution curve reaches 0.3μm which is the minimum measurable diameter for the LALLS instrument. The volume based mean diameter is 5.0μm and the corresponding number based mean diameter is 1.5μm. The CC powder exhibits a peak at 3μm and appears to have narrower size distribution than HS powder. Its volume based mean diameter is 5.7μm and corresponding number based mean diameter is 2.8μm. The larger mean diameter of the CC powder is consistent with the SEM analysis. However, mean diameter of both HS and CC are slightly above expected values. Also, the steep curve at the lower end of the grade CC PSD is not as expected since particles below 1 μm are observed in the SEM analysis.

Used CIP grade HS was also measured after $8 \cdot 10^5$ cycles of real-world usage in a prosthetic knee joint (not shown in figures). The used powder was expected to show an offset towards smaller particles when compared to unused powder. On the contrary, the results showed an increase in mean particle size. There can be various reasons for these unexpected results. The two samples do not origin from the same batch of CIP. Therefore, variations in PSD between batches from the producer can affect the results. The difference in morphology between used and unused powder can have a large effect on the results. In the measuring technique, all particles are assumed to be perfectly spherical. This is a good approximation for unused powder but not as good for the used powders (see Figure 4.4). The flake-shaped particles tend to agglomerate and can be measured as larger particles. Yet another possible cause for unexpected results may be a selective sampling method. A bottle containing CIP in a solvent is shaken and stirred until it shows a uniform colour. A portion of the solvent containing CIP is then poured into another bottle or onto a sample holder. More advanced methods could be used to eliminate the possibility of selectivity.

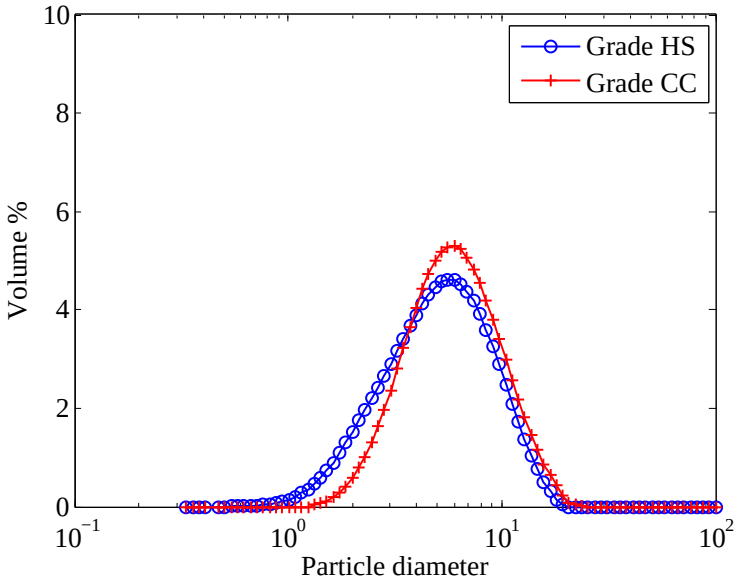

Figure 4.9: Volume based PSD for unused CIP

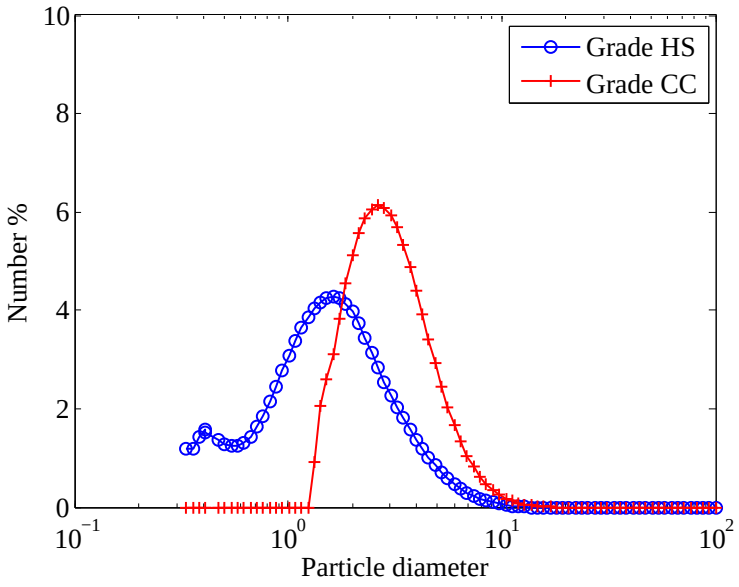

Figure 4.10: Number based PSD for unused CIP

4.6 Magnetization characteristics

The magnetic characteristics for unused CIP of grades HS and CC are measured with a Vibrating Sample Magnetometer (VSM). The measurements are performed in a laboratory in Brazil under the supervision of Prof. Antonio Bombard (UNIFEI (2011)). The magnetization curves for unused HS and CC powder are shown in Figure 4.11. Grade CC powder exhibits higher saturation than grads HS, which corresponds to the higher content of iron. The saturation of grade CC is 210 emu/g while the saturation of grade HS is 139 emu/g. Grades HS and CC are saturated at a similar field strength of approximately 10^4 Oe.
Attempts are made to measure the magnetization curves for used CIP, both using VSM and a Superconducting Quantum Interference Device (SQUID). The measurements are performed by professionals in two different countries but neither of them returned plausible results. The reason for that remains unknown. When this is written, new samples are being sent abroad to re-measure the magnetization of used CIP using VSM.

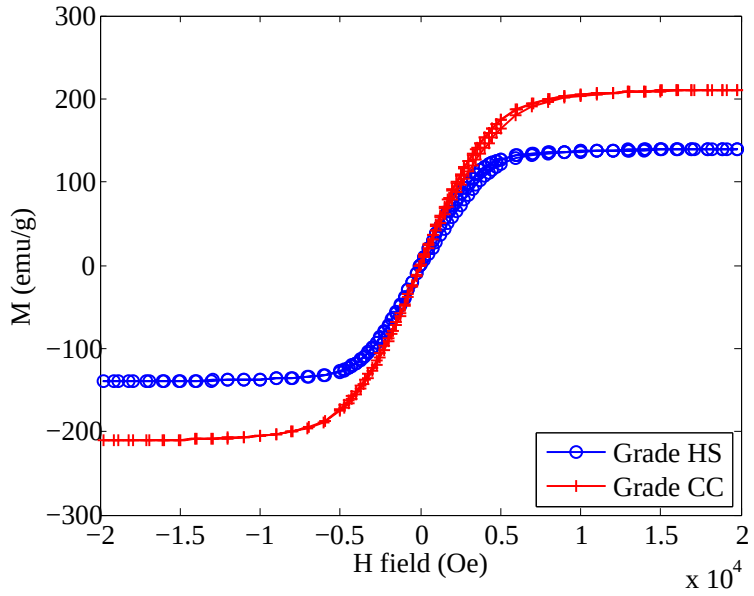

Figure 4.11: Magnetization curves for grade HS and CC particles

5 Conclusions

Durability of the prosthetic knee joint is shorter than its expected lifetime stated by the device patent. This is mainly due to degradation of the MR fluid in the device, such as the well known in-use-thickening. Mechanical energy dissipated by the fluid over this stated lifetime is above recognized threshold for the durability of MR fluids. Energy dissipated in the actual lifetime of the fluid is however approximately 50% below this threshold. At first glance this may seem like a poor durability since the most durable MR fluids today take up twice as much energy in their lifetime. For this application however, only a small increase in off-state torque makes the device fail the design constraints. Even after taking up twice this energy the actuator can easily be cycled and the brake appears to work fine. The used MR fluid may still be usable in other applications. The constraints are very strict but necessary to ensure comfort for the amputees using the prosthetic device. It is also noticed that the durability limit proposed by Carlson is not specific for direct shear-mode devices. The MR prosthetic actuator is a direct shear-mode device with high shear rates. Taking all of this into account, half of the energy dissipation of the most durable MR fluids today must be considered as a very good durability.

Measuring the off-state torque at varying temperatures and using the criteria for minimum swing extension indicates that the minimum ambient temperature for a new knee joint to function normally is 11°C. Measuring the on-state torque for varying coil current from 0 to 2 Ampers confirms what had been calculated theoretically before; that increase in torque with increased current is very small or negligible above 1.5A. Durability tests performed indicate in-use-thickening of the fluid at a linear rate. In addition to the increase in off-state torque with number of cycles the on-state torque decreases as well, lowering the turn-up ratio at an even faster rate.

The main mechanism responsible for the degradation of the fluid appears to be fracturing and spalling of the particle surface when subjected to prolonged high shear stresses. This causes thin flakes of iron to peel away from the surface. The flake-shaped secondary particles are believed to agglomerate, resulting in increased fluid viscosity over time. This change in particle morphology is also believed to be the main mechanism responsible for decreased on-state shear stress. Theoretically, the flake-shaped particles exhibit poorer magnetic properties than spherical ones, besides having a lower packing factor.

Flakes from the inner- and outer housing of the actuator are observed in the fluid. This is the result of mechanical scuffing between the steel blades and inner- and outer housing. Nano-sized particles, which also can drastically increase the fluid viscosity, are not observed in the fluid as suspected at the beginning of the project. Elemental analysis does not indicate oxidation at a measurable degree in the MR fluid.

The brittle surface and onion-skin structure of mechanically hard unreduced CIP is believed to contribute to the formation of thin flakes in used fluids. Tests indicate however that mechanically soft reduced CIP exhibits poorer durability than mechanically hard particles for this application. The high shear stresses cause the mechanically soft particles to deform severely and agglomerate, resulting in paste formation of the fluid. The silica coating on the particles may however be partly responsible for the paste formation. Friction reducing additives are tested with mechanically hard particles as an attempt to decrease the particle spalling. This also results in decreased durability compared to the currently used fluid composition. It is believed that the PFPE base fluid and dispersion additive have better lubricating properties than the friction reducing additives tested.

After years of development, the MR fluid in this application exhibits good quality with respect to both magnetorheological performance and durability. However, it is the believe of the author that improvements for the proposed MR fluid, with regards to durability, can be achieved with further innovations.

References

BASF (2010). *BASF Corporation.*

BASF (website). Basf corporation, August 2010. URL `http://www.basf.com/group/corporate/en/`.

J. D. Carlson. What makes a good mr fluid? *J. Intell. Mater. Syst. Struct.*, 13:431–435, 2002.

J. D. Carlson. Critical factors for mr fluids in vehicle systems. *International Journal of Vehicle Design*, 33(1-3):207–217, 2003.

C. T. Crowe, D. F. Elger, and J. A. Roberson. *Engineering Fluid Mechanics, 8th ed.* John Wiley & Sons, Inc., 2005.

S. Cutillas, G. Bossis, and A. Cabers. An experimental investigation of unimodal and bimodal magnetorheological fluids with an application in prosthetic devices. *Phys. Rev. E*, 57(1):804–811, 1998.

DuPont (2011). *DuPont Corporation*.

G. A. Flores, J. Liu, M. Mohebi, and N. Jamasbi. Field-induced columnar and bent-wall-like patterns in a ferrofluid emulsion. *International Journal of Modern Physics B (IJMPB)*, 13(14-16):2093–2100, 1999.

R. T. Foister, V. R. Iyenger, and S. M. Yurgelevic. Low-cost mr fluids with powdered iron, 2004.

E. M. Furst and A. P. Gast. Dynamics and lateral interactions of dipolar chains. *J. Intell. Mater. Syst. Struct.*, 62(5), 2000.

M. A. Golden, J. C. Ulicny, K. S. Snavely, and A. L. Smith. Magnetorheological fluids, 2005.

K. H. Gudmundsson, F. Jonsdottir, F. Thorsteinsson, and O. Gutfleisch. An experimental investigation of unimodal and bimodal magnetorheological fluids with an application in prosthetic devices. *J. Intell. Mater. Syst. Struct.*, DOI: 10.1177/1045389X11403821, 2011.

J. Harris. *Rheology and Non-Newtonian Flow*. 1977.

H. Hsu, C. R. Bisbee, M. L. Palmer, R. J. Lukasiewicz, M. W. Lindsay, and S. W. Prince. Magnetorheological fluid compositions and prosthetic knees utilizing same, 2006.

Innovation Center Iceland (2011). *(Nýsköpunarmiðstöð Íslands)*.

V. R. Iyengar and R. T. Foister. Durable magnetorheological fluid compositions, 2003.

V. R. Iyengar, R. T. Foister, and J. C. Johnson. Mr fluids containing magnetic stainless steel, 2004.

F. Jonsdottir and K. H. Gudmundsson. Bidisperse perfluorinated polyether (pfpe)-based magneto-rheological fluids in a prosthetic knee. In *ASME Conference Proceedings*.

F. Jonsdottir, E. T. Thorarinsson, H. Palsson, and K. H. Gudmundsson. Influence of parameter variations on the braking torque of a magnetorheological prosthetic knee. *J. Intell. Mater. Syst. Struct.*, 20(1):659–667, 2009.

T. J. Karol, B. C. Munoz, and A. J. Margida. Magnetorheological fluid, 1999.

D. J. Klingenberg, C. H. Olk, M. A. Golden, and J. C. Ulicny. Effects of nonmagnetic interparticle forces on magnetorheological fluids. *Journal of Physics: Condensed Matter*, 22(32), 2010.

B. C. Munoz. Magnetorheological fluid, 1997.

B. C. Munoz, A. J. Margilda, and T. J. Karol. Organomolybdenum-containing magnetorheological fluid, 1997.

Nye (2011). *Nye Lubricants, Inc.*

R. E. Rosensweig. Magnetic fluids. *Ann. Rev. Fluid Mech.*, 19:437–463, 1987.

S. Shahinpoor and H.-J. Schneider. *Intelligent Materials*. RSC Publishing, 2008.

A. L. Smith, J. C. Ulicny, and L. C. Kennedy. Magnetorheological fluid fan drive for trucks. *J. Intell. Mater. Syst. Struct.*, 18:1131–1136, 2007.

Össur hf. (2011). *Össur Corporation*.

E. T. Thorarinsson. Analysis of a magnetorheological prosthetic knee. M.Sc. thesis, Faculty of Engineering, University of Iceland.

J. C. Ulicny, A. L. Smith, M. A. Golden, and C. A. Hayden. Magnetorheological fluids with stearate and thiophosphate additives, 2005.

J. C. Ulicny, M. P. Balogh, N. M. Potter, and R. A. Waldo. Magnetorheological fluid durability test - iron analysis. *Mater. Sci. Eng. A*, 443(1-2):16–24, 2007a.

J. C. Ulicny, C. A. Hayden, P. M. Hanly, and D. F. Eckel. Magnetorheological fluid durability test – organics analysis. *Mater. Sci. Eng. A*, 464(1-2):269–273, 2007b.

UNIFEI (2011). *Itajubá Federal University Brazil*.

Vanderbilt (2011). *R.T. Vanderbilt Company, Inc.*

K. D. Weiss, D. A. Nixon, J. D. Carlson, and A. J. Margida. Thixotropic magnetorheological materials, 1995.